MAGNETIC LENS SPECTROMETER INVESTIGATIONS OF GAMMA-RADIATION FROM LIGHT NUCLEI

Thesis by

Robert James Mackin, Jr.

In Partial Fulfillment of the Requirements

For the Degree of

Doctor of Philosophy

California Institute of Technology

Pasadena, California

1953

ACKNOWLEDGMENTS

The author is grateful to Professor T. Lauritsen for guidance and encouragement throughout the course of his work. He is also indebted to Professors W. A. Fowler, R. F. Christy, R. P. Feynman, and C. C. Lauritsen, for their continued interest and for much valuable advice. He would like to thank Dr. R. G. Thomas for instruction in the art of gamma-ray spectroscopy; and Mr. W. R. Mills, Dr. W. B. Mims, and Dr. C. Wong, for assistance with experiments and calculations.

The assistance of a National Science Foundation Predoctoral Fellowship during the last year is gratefully acknowledged. The experimental work was assisted by the joint program of the Office of Naval Research and the Atomic Energy Commission.

ABSTRACT

A magnetic lens spectrometer has been used in conjunction with an electrostatic accelerator to study gamma-radiation produced by light-nuclear reactions. The apparatus and techniques for its use are described. Formulas are given which are used in analyzing the data.

A radiative transition in Li^6, produced by the (resonant) reaction $Be^9(p,\alpha)Li^{6*}$ was studied in detail. The gamma-ray energy was found to be 3.572 ± 0.012 Mev, not correcting for a 0.026-Mev Doppler shift. The internal pair spectrum was strong evidence that the transition proceeded by magnetic dipole (M1) radiation, but electric quadrupole (E2) was not finally excluded. Capture radiation from the same resonance has energy 8.1 ± 0.2 Mev and is 10^3 times less intense.

The internal pair spectrum from the first excited state of Be^{10} (produced by $Be^9(dp)Be^{10*}$) showed the radiation to be E2. The internal pairs from the 3.60-Mev transition of B^{10} exclude E1 for that radiation. Gamma-rays assigned to B^{10} were measured (without Doppler correction) as 3.595 ± 0.014, 4.44 ± 0.03, and 5.98 ± 0.04 Mev. The last named was assigned to the 5.93-Mev level of B^{10}.

Gamma-rays produced by $C^{12} + D^2$ have energies 3.843 ± 0.014, 3.684 ± 0.020, and 0.1682 ± 0.001 Mev. On the basis of data presented, the first two are assigned to levels of those energies in C^{13} and the last as a transition between them. Arguments are given that the presence of this low-energy transition, in conjunction with other data, assigns spins 5/2, even, and 3/2, odd, to the respective levels. The internal pairs agree with M2 for the higher-energy radiation but definitely exclude only E1. Internal pair data for the 3.68-Mev transition is inconclusive, but suggests E2 or E1.

TABLE OF CONTENTS

TABLE OF CONTENTS (Cont'd)

I. INTRODUCTION

A. GENERAL

This thesis describes a series of investigations of gamma-rays produced by the bombardment of light nuclei. It reports a number of experimental results which show little evidence of interrelatedness. Actually, the unifying thread is to be found in Professor T. Lauritsen's voluminous compilation of the data concerning energy levels of light nuclei. The present effort has added a few details to the picture emerging from his work.

In particular, this type of study delineates certain properties of low-lying excited states, less readily approached by scattering experiments. These are the levels whose features must eventually be described by some nuclear model, and the accumulation of data has very nearly reached the point where a detailed comparison will be possible.

B. APPARATUS AND TECHNIQUES

A magnetic lens spectrometer was used to study the spectrum of secondary electrons produced by gamma-rays originating at its source point. From such spectra can be inferred the gamma-ray energy to a few tenths of one percent, the intensity of the gamma-ray to around ten percent, and sometimes its internal conversion coefficient (pair or K-electron).

As regards energy measurements, the spectrometer has a powerful competitor in the rapidly developing scintillation spectrometer. That instrument possesses the twin advantages of extremely high sensitivity and comparative ease of operation. The lens spectrometer can offer in its defense better resolution, leading to greater accuracy and increased ability to detect weak lines in the presence of strong radiation. A case in point is the high energy (capture) radiation from protons on beryllium (II, D) which was inundated, in the scintillation spectrometer, by the thousand times stronger radiation following the competing $Be^9(p,\alpha)Li^{6*}$ reaction. Another virtue is the spectrometer's relative insensitivity to a neutron background which would incapacitate a scintillation counter. It will be apparent later (III) that the lens spectrometer is not entirely perfect in this respect, however.

As a practical device for measuring an internal conversion coefficient, the magnetic spectrometer is unmatched. The relation between this number and a gamma-ray's multipolarity is well established (I, E), and thus the latter, more interesting, quantity is determined by such a measurement. Angular distributions and correlations of reaction products frequently lead to ambiguities in level spin assignments. Gamma-ray multipolarities resolve these and often lead to unique spin assignments independent of other data.

The general design of the instrument (shown in Figure 1) and its application to gamma-ray energy measurements are described by Hornyak, Lauritsen, and Rasmussen[1]. For more details on construction techniques, the reader is referred to the theses of the first and third authors[1bc].

The analysis of experimental data is simplified by the following features:

1. The spectrometer contains no iron; the magnetic field, and thus the momentum of focussed particles, is directly proportional to lens current. A helical baffle separates positron and electron components.

2. The resolution curve (spectrum of a monoenergetic electron source) has been made very nearly a gaussian of constant fractional *momentum* width. For the experiments described below, this width was 1.9 percent, as measured by the thorium F, I, and X internal conversion lines.

3. The background of detector counts consists mostly of scattered electrons, Comptons produced by gamma-rays striking baffles visible from the source, and sometimes high energy neutrons; it is very nearly independent of spectrometer current.

4. For gamma energies above a few hundred kilovolts a scintillation counter detector was used. It employed a trans-stilbene crystal (1-inch cylinder, 1 inch long), 18-inch lucite light pipe, and RCA 5819 phototube, mounted in a solenoid which balanced out the spectrometer field. This apparatus is described in detail in C. Wong's thesis(2), but a few remarks on its usefulness are not amiss here. For a given current setting, the focussed electrons produced an integral bias curve (plot of counts with amplified pulse heights greater than a certain bias voltage, versus the bias voltage) with an accurately flat plateau and a well-defined point of departure. It was thus possible to set the discriminator to the highest bias consistent with counting all of the electrons of interest and thereby minimize the background counts. This feature made possible the detection of certain high

energy gamma-rays which would have been missed otherwise, and considerably improved experimental results where high background had made a statistical shambles of data taken with a Geiger counter. It also made it possible to insure that certain weak "spectra" had the energy represented by the lens current and that others were spurious. (See IV, G, and Wong's thesis[2]). The thousand-fold higher count rate possible because of shorter dead-time represented a convenience not available with the Geiger counter.

In the experiments to be described, a beam of bombarding particles produced by Kellogg Radiation Laboratory's 3-Mv electrostatic accelerator was magnetically analyzed to an energetic homogeneity of about 0.1 percent and focussed on a target in the spectrometer vacuum-chamber. Figure 1 shows the spectrometer and the experimental geometry.

The target holder was insulated to allow measurement of beam current, and measured spectra were ordinarily normalized on the charge collected by means of a standard current integrator accurate to one percent. Precision required the usual special precautions to insure that only the incident beam contributed to the current (viz., a negatively charged electron-suppressor ring, and a positive potential on the target). In addition, the beam was monitored with a shielded Geiger counter or Geiger telescope which recorded the total gamma-ray yield from the reaction. For non-conducting targets which emitted positive ions under bombardment (soot, boron), the latter was the only means of normalization.

A target was customarily several thousandths inches thick - enough to stop the impinging beam - and was mounted on a disk or foil of converter material, aluminum or copper. If a photoelectron spectrum was desired, a thin thorium foil was pasted on the backing material with vacuum grease. For convenience, nearly all targets and converters were made the same diameter - 0.375".

More information on techniques will be found in the descriptions of individual experiments. A detailed summary of experimental procedures in beta-spectroscopy will be found in a monograph by C. Sharp Cook[4].

C. GAMMA-RAY ENERGY MEASUREMENTS

The calibration constant relating momentum and lens current was determined by measuring the spectrum of internal conversion electrons from Thorium B and C". The best values (in gauss-cm) for the momenta of the principal lines are: X, 9988.4 ± 2, Brown[5]; I, 1754.01 ± 0.25, Lindström[6]; F, 1388.55 ± 0.20, Lindström[6].

A different constant was determined by comparing each line momentum with the lens current corresponding to the peak of its gaussian and the results averaged. The internal consistency was better than 0.1 percent, and the distribution of values, judging from several measurements, was random. For all measurements, it was necessary to correct for the horizontal component of the earth's magnetic field, which lay along the spectrometer axis. (The vertical component was balanced out with a pair of Helmholtz coils.) The correction was 5.3 gauss-cm, determined by observing the shift of the F-line with reversal of lens current (sans helical baffle).

A photoelectron spectrum from a thin converter most nearly approximates an internal conversion line as being monoenergetic; that is, the measured spectrum is a near-gaussian curve only slightly broader than the spectrometer resolution. For this reason, and because internal conversion lines are notoriously weak for light nuclei, it gives the most precise possible indication of gamma-ray energy wherever the photoelectric cross-section is large enough to produce a measurable spectrum. This includes energies up to 3.5 Mev, roughly. The Z^5 dependence of the cross-section (for energies customarily encountered) suggests a heavy element converter; thorium has been used in Kellogg Laboratory almost exclusively, because of ease in handling.

To the photoelectron energy it is necessary to add the atomic binding energy of thorium to find the gamma energy. For the K-shell this is 109.63 kev, according to the recent work of Cauchois[(7)]; a summary of binding energies is given by Hill, Church, and Mihelich[(7b)].

A further small correction is the photo-peak shift caused by electron energy losses in the converter. This can be determined from a graph given by Hornyak, et al.[(1)] which is based on a study by Christy and Cohen.

For gamma-rays of higher energies, the Compton spectrum provides the necessary information. The peaked spectrum from a thin converter is employed where intensity is sufficient. One technique of analysis utilizes the spectrum of a known gamma-ray from a converter of equal thickness to find a relative energy. Close similarity between the spectra makes an overall comparison possible and produces an accuracy comparable to that resulting from a photopeak measurement (IV, B). An alternative technique consists of the comparison of experimental curve and a theoretical spectrum. The difficulties encountered in this procedure are related in the Appendix to Part II.

For weaker gamma-rays, or where a yield measurement is of interest, the thick converter Compton spectrum is studied. Either mode of analysis is applicable, the latter being somewhat more convenient. (See III, B). For reasons not altogether understood, the energy values resulting from theoretical comparisons are uniformly 1.006 times the true values. In the Appendix to II, this is documented, and possible reasons for it are given.

In no case was it found necessary or profitable to make an energy or intensity measurement from a pair spectrum.

Finally, it must be remembered that when a gamma-ray is produced in a nuclear reaction, it may be emitted by a moving nucleus, and its apparent energy will depend on this motion. Thus, Doppler effects may produce both a broadening and a shift of the measured spectrum. Their presence constitutes a statement that the lifetime for gamma emission is less than the time required for the residual nucleus to be appreciably slowed in the surrounding material. When it is not clear whether this occurs, an extra uncertainty in the energy measurement prevails. Quantitative estimates of the effect are given by Thomas[3].

D. GAMMA-RAY YIELD MEASUREMENTS

This section is based on the work of Thomas and Lauritsen[3]; it lists several formulas which are used in the analysis of the experiments described in the following sections. The analysis consists of comparing the experimental spectrum of Compton electrons with a theoretical one based on the well-established Klein-Nishina cross-section. Only the upper 5 or 10 percent is compared, leading to much simplification.

The spectrum of detector counts as a function of electron momentum, $S(B\rho)$, produced by a monochromatic gamma-ray source of (isotropic) yield Y in an infinitely thin converter is

$$S(B\rho) = Y\pi r^2 k^{-1} \, Nt \, \langle \sec \theta \rangle \Omega \, \mathcal{F}_1 \left[f(x) \right] \frac{dx}{dB\rho} \tag{1}$$

where

πr^2 is the cross section of a classical electron, 0.250×10^{-24} cm^2.

k is the gamma-ray energy in units of mc^2, the electron rest energy.

Nt is the number of electrons contained in a square centimeter of the converter.

$\langle \sec \theta \rangle \Omega$ reflects the influence of converter geometry on the spectrum. $\langle \sec \theta \rangle$ is the average secant of the (polar) angle of emission of gamma-rays which produce electrons accepted by the spectrometer. Ω is the effective acceptance solid angle (including transmission factors and counting efficiency) expressed as a fraction of a sphere. The precise treatment of the conversion process gives an expression for this product which cannot be separated. For gamma-rays of energy greater than 2 Mev, however, it is sufficiently accurate to regard the recoil electron as being propelled straight forward by the gamma-ray so that θ is just the mean acceptance angle of the spectrometer (20°). (For 2-Mev gamma-rays, the upper 5 percent of the Compton spectrum is inside a cone of half-angle 8°.) A consequence for anisotropic gamma-rays is that Y is 4π times the yield per unit solid angle at the acceptance angle.

$$f(x) = \frac{1}{k^2 x^2} + \frac{k^2 - 2(1+k)}{k^2 x} + x + \frac{1+2k}{k^2} \qquad \left[x \geq \frac{1}{1+2k}\right]$$
$$= 0 \qquad \left[x < \frac{1}{1+2k}\right] \tag{2}$$

is the electron energy spectrum as given by the Klein-Nishina formula in terms of $x = 1 - T/k$; T is the electron kinetic energy in units of the electron rest energy. $\pi r^2 f(x)\, dx/k$ is the Klein-Nishina differential cross-section. The angle between the electron's momentum and that of the incident gamma-ray is ω:

$$\sin^2\omega = \left[x(1+2k) - 1\right] / \left[k^2 (1-x) + 2k\right].$$

$\mathfrak{F}_1$ is an operator representing the fold of the spectrum with the spectrometer resolution curve. For the Kellogg instrument, the curve is a gaussian, $\exp\left[-(1.67\, \Delta B\rho / pB\rho)^2\right]$, where $\Delta B\rho$ is the departure from a given momentum setting, $B\rho$, and $pB\rho$ is the full width at half-maximum of the resolution curve at that setting.

$dx/dB\rho = 0.300\, \beta / kmc^2$, mc^2 in kev, $B\rho$ in gauss-cm, is the conversion ratio between the energy and momentum scales. β, the electron velocity in units of the speed of light, is taken as constant; an average value is used.

The redistribution of the electron spectrum due to distributed energy losses in the converter has been studied, for our geometry, by Thomas and Lauritsen on the basis of work by N. Bohr(8), A. Bohr(9), and L. Landau(10), and I summarize their findings. The most probable energy loss for electrons passing through matter along a path of length ℓ is

$$\Delta E = \mu \ell = B\ell \left[\log(2B\,\ell\, mc^2\beta^2\gamma^2/I^2) - (1-F_p)\beta^2 + 0.37\right] \qquad (3)$$

where

$B = 2\pi N r^2\, mc^2/\beta^2$; $\gamma = (1-\beta^2)^{-1/2} = 1 + T$;

I ($= I(\gamma)$) is the average excitation potential of the matter traversed including polarization effects (which introduce the γ-dependence);

F_p is the fraction of atomic electrons which are essentially bound by polarization forces (due to the presence of nearby atoms in the medium).

From a semi-empirical expression for the frequency distribution of the quantum-mechanical oscillators of aluminum (the usual converter material), there results the numerical expression

$$\mu(\text{kev/mg/cm}^2) = 0.0741\,\beta^{-2}\left[\log F_p \ell/a + (1-F_p)\beta^2 + 0.37\right] \qquad (4)$$

where

$$F_p = \left[(1 + 0.195\gamma^2)^{1/2} - 1\right] / \left[(1 + 0.195\gamma^2)^{1/2} + 1\right]$$

a is the radius of the first Bohr orbit of an H atom, 0.529×10^{-8} cm.

This formula deviates less than one percent from an evaluation of μ employing x-ray absorption data[11] to find the oscillator distribution. It gives values of μ which agree strikingly well (2 percent) with recent experimental determinations of Chen and Warshaw[12], and Kageyama and Nishimura[13], for energies between 500 kev and 2 Mev. It is convenient to remember that above 4 Mev, nearly all oscillators are polarized; $F_p = 1$ gives μ to within 3 percent for $\ell > 5$ mg/cm^2. A handy figure for estimates is $\mu \sim 1$ kev/mg/cm^2, since the first factor in (4) is between 0.06 and 0.08 for most materials.

If we symbolize the effect of the energy loss distribution by operating on f(x) with $\mathcal{F}_2$, then

$$\mathcal{F}_2 \left[f(x)\right] = \frac{kmc^2}{\mu \ell} \int_{(1+2k)^{-1}}^{x} \Phi \left(\frac{kmc^2(x-x')}{\mu \ell}, \frac{\mu}{B} + 0.05\right) f(x')dx' \qquad (5)$$

where the kernel Φ is a function derived from the theoretical loss distribution of Landau[10]. It is nearly constant for values of the first argument (call it ξ) less than one (i.e., for energy losses less than the most probable) and falls off roughly as $(\xi - 0.75)^2$ for larger values. The second argument is a parameter depending on a mean value of the electron energy. The Landau function gives the electron spectrum resulting when a monoenergetic beam passes through a foil. The derived function, Φ, describes the spectrum when such electrons originate uniformly throughout the foil. Their relationship is given in Reference 3. The derivation of (5) makes use of μ's slow variation with path length.

An infinitely thick converter is defined as one for which $\xi < 1$ for the maximum interesting value of x. For this case,

$$\mathcal{F}_2\left[f(x)\right] = \frac{kmc^2}{\mu \ell}\, \Phi\left(0, \frac{\mu}{B} + 0.05\right) \int_{(1+2k)^{-1}}^{x} f(x')dx'$$

$$\equiv \frac{kmc^2}{\mu_e \ell} F(x)$$

$$F(x) = \int_{(1+2k)^{-1}}^{x} f(x')dx' \qquad (6)$$

$$= \frac{2}{k} - \frac{1}{2(1+2k)^2} + \frac{(1+2k)x}{k^2} + \left(1 - \frac{2}{k} - \frac{2}{k^2}\right) \log (1+2k)x + \frac{1}{2}x^2 - \frac{1}{k^2 x}$$

$$\Phi\left(0, \frac{\mu}{B} + 0.05\right) = 0.765 + 0.0058\left(\frac{\mu}{B} + 0.05\right)$$

μ_e is called the effective stopping force.

In the application of $\mathcal{F}_2$ to the expression (1), the quantity ℓ may be taken to equal t $\langle \sec \theta \rangle$. This ignores the increase in path length caused by multiple scattering, the so-called umweg factor. As it happens, the angular redistribution of electrons by multiple scattering cancels this effect to first order, and no correction is made.

F(x) is a fairly smooth function. Accordingly, away from the end point its curvature may be neglected and the window fold may be approximated:

$$\mathcal{F}_1\left[F(x)\right] = 1.064\ pB\rho\, F(x)$$

Thus, for an infinitely thick converter

$$S(B\rho) = Y\Omega N\pi r^2 \frac{mc^2}{\mu_e}\, 1.064\ pB\rho\, \frac{dx}{dB\rho}\, F(x) \qquad (7)$$

In practice, the top 5- or 10-percent of this spectrum is plotted, with mean values for the slowly varying quantities μ_e and $dx/dB\rho$. The tail at the end-point of the spectrum is estimated (or computed by numerical evaluation of $\mathcal{F}_1\left[F(x)\right]$. A best fit with the experimental spectrum is obtained to determine the value of $Y\Omega$. Ω is determined by following the same procedure with a Co^{60} source for which Y is known.

The procedure has been streamlined, somewhat. Lumping parameters, we may write

$$Y\Omega = A(k)S(B\rho)/F(x) \tag{8}$$

A(k) may be identified by comparison of the two expressions for $S(B\rho)$. It is plotted in Figure 2.

An example is the yield measurement of the three gamma-rays from $F^{19}(p, \alpha)O^{16*}$. The target was a 0.035-inch CaF^2 crystal, and the converter a 0.825 g/cm^2 Al disk. A very fine nickel wire touched the crystal near the beam spot to avoid charge accumulation and insure complete current collection. Bombarding energy was 1 Mev; each run corresponded to 14.4 microcoulombs, and about one third were repeated up to three times.

The spectrum is shown in Figure 3. The solid curves are plots of the corresponding theoretical expressions (Eqn. 7). The background under the 6.13-Mev line is based on data taken at lower spectrometer currents and the assumption that all three lines produce similar spectra. The nuclear pair yield from the 6.05-Mev level, being down by a factor of a thousand, affects this estimate only slightly.

The resultant energies and yields are

6.12 ± 0.05 Mev	5.56×10^{-7} γ/p
6.89 ± 0.08 Mev	0.72×10^{-7} γ/p
7.08 ± 0.08 Mev	1.10×10^{-7} γ/p

The total yield, 7.38×10^{-7} γ/p, differs by only 5 percent from the older value(14)(15), 7.03×10^{-7} γ/p, derived from work at Kellogg Laboratory. Accounting for the anisotropic distribution of the 6.9 and 7.1 lines at the 873 kev resonance(16) brings the two figures even closer together. The difficulty of this experiment and the poor statistics on the lines in question preclude any claim to even 5 percent accuracy, however.

Plainly, much of the uncertainty in such a yield measurement lies in the computation of the effective energy loss μ_e. Two factors inhibit the use of the thin-converter spectrum in avoiding this difficulty. Foremost is the ten-fold decrease in the count rate when a converter is used whose thickness is comparable with the spectrometer resolution width. The other results from the target's contribution to the Compton spectrum. A target "thick" for an incident deuteron beam has a thickness equal to a large fraction of a resolution width for secondary electrons. Using target as converter presents the difficulty of assigning a converter thickness when not all gamma-rays originate at the surface. Solving this by measuring, then subtracting two spectra with slightly different converter thicknesses presents additional problems, the chief one again being intensity.

The thin-converter photoelectric spectrum does not suffer from this handicap. The Z^5 cross-section dependence assures that the entire spectrum will be produced in the thorium foil appended to the target backing. Because the photo-electrons are produced in a finite momentum range it is adequate and convenient to compute only the integral of the measured spectrum. The variation of window width suggests dividing each point by its corresponding momentum reading before integrating. A fairly rigorous derivation gives:

$$Y\Omega \sigma N_a t \langle \sec \theta \rangle = \frac{1}{1.064p} \int_0^\infty S(B\rho) \frac{dB\rho}{B\rho} \qquad (9)$$

where all terms are as defined under (1) except:

σ is the total K-shell photo-electric cross-section, given to better than 5 percent at two energies by the numerical computations of Hulme et al.[17] (they neglect only electron exchange and outer shell screening) and continued to other energies by H. Hall[18] and L. H. Gray[19] (semi-empirical);

$N_a t$ is the number of atoms per square centimeter of converter; and

$\langle \sec \theta \rangle$ depends on the angular distribution of the photoelectrons.

The last-named factor is the major cause of uncertainty in the yield determination. The nearest approach to a rigorous computation is that of Sauter[20] who performs a relativistically exact Born-approximation calculation of the angular distribution. Extended and fruitless experiments by R. Thomas[3b] and the author have demonstrated the folly of using Sauter's equation for thorium converters.

It was decided to determine $\langle \sec \theta \rangle$ empirically, using a series of sources of known strength and maintaining a constant source geometry. The configuration used consisted of a 3/8" diameter flat converter at 1/16" from the source; it was one for which previous experiments had shown that $\langle \sec \theta \rangle$ was independent of converter thickness. The empirical determination of $\langle \sec \theta \rangle$ also removes the residual uncertainties resulting from inaccuracies in the total cross-section.

Equation (9) may be placed in a form convenient for analyzing experimental data:

$$Y\Omega = \frac{1}{t\langle\sec\theta\rangle} B(k) \int_0^\infty \frac{(B\rho)_o}{B\rho} S(B\rho)\, dB\rho \qquad (10)$$

where

t is the thorium converter thickness in mg/cm^2,

B(k) may be found by comparing (10) with (9), and

$(B\rho)_o$ is the momentum of the K-peak; in most cases $(B\rho)_o/B\rho$ may be taken as 1. B(k) and the empirical values of $\langle\sec\theta\rangle$ are plotted in Figure 4.

E. INTERNAL CONVERSION COEFFICIENTS

1. K-electron Coefficient

Thomas[3] attempted to measure internal K-coefficients for two light-nuclear gamma-rays. The effect was so small that his results were inconclusive. The insignificance of the effect stems from its dependence on Z^3. No K-shell internal conversion coefficients are reported in this thesis. For the record, accurate relationships between gamma-ray multipolarity and internal conversion coefficients are given by Rose et al[21]. See Thomas and Lauritsen[3] for a summary of the experimental problems which arise in the measurement.

2. Pair Coefficient

Much more feasible for light-nuclear transitions is the measurement of the fraction of de-excitations of a level which occur by the emission of an electron-positron pair. To first order (Born approximation) the process is independent of Z; in fact, it is just for low-Z elements that the Born approximation gives a reasonably correct relationship between gamma-ray multipolarity and internal pair coefficient. The problem has been solved with this approximation by Rose[22], who has given the momentum distribution as well as the total coefficient. It is this distribution which is useful in analyzing beta-spectrometer data, inasmuch as most reactions produce complex gamma-spectra, and each pair-distribution can be measured only at the high energy end.

In most experiments it is obviously more practical to measure the positron spectrum. Rose's general expression for this has been evaluated by Thomas[3b] for several multipoles in terms of gamma-ray energy k, positron and electron momentum, p_+ and p_-, and total energy, W_+ and W_-, all in units of mc^2. A form more convenient for actual computations follows.

Per quantum of electric or magnetic radiation of multipole order ℓ, the number of positrons with momentum in the range dp_+ at p_+ is

$$\Gamma_{\substack{E\ell \\ (M)}} (p_+)\, dp_+ = \frac{1}{137\pi k^3}\, \beta_+\, Q_{\substack{E\ell \\ (M)}} (p_+)\, dp_+ \tag{11}$$

Let

$$x = W_+ W_- \qquad y = p_+ p_-$$

$$b = (1+x+y)/k.$$

(Note the identity: $(x+1)^2 = k^2+y^2$.)

Then the first few Q's, in order of decreasing magnitude, are:

$$Q_{E1} = (k^2 - 2x \quad) \log b + 2y$$
$$Q_{E2} = (k^2 - 2x - 2) \log b + 8y(x-1)/3k^2$$
$$Q_{M1} = (k^2 - 2x - 2) \log b \qquad (12)$$
$$Q_{E3} = (k^2 - 2x - 4) \log b$$
$$-2y\left[1-3(3x-1)/2k^2-2(3x+3-y^2)/k^4\right]$$
$$Q_{M2} = (k^2 - 2x - 4) \log b - 2y\left[1-3(x+1)/k^2\right]$$

This notation stresses the identity of electron and positron spectra which one would expect to emerge from the Born approximation; or, what is the same, the symmetry of each spectrum about its midpoint.

In the unlikely event that higher multipoles are to be computed a recursion formula should be used. Define

$$z_o = -2 \log b$$
$$z_\ell = \left[(1-2b/k+4y/k^2)^\ell - (1-2b/k)^\ell\right]/\ell$$

Then:

$$Q_{E(\ell+1)} = Q_{M\ell} + 2\frac{\ell+1}{\ell+2}\left[(k^2/4)\, z_{\ell+1} - (k^2/4-x)z_\ell\right]$$
$$Q_{M(\ell+1)} = 2Q_{M\ell} - Q_{M(\ell-1)} - (k^2/4)z_{\ell+1} + (x+1)z_\ell + (k^2/4-x)z_{\ell-1} \qquad (13)$$

Beginning with Q_{E1}, Q_{M1}, and Q_{M2}, all multipoles can be computed. Recurrent factors in the recursion formulas make their application less formidable than their appearance.

Most of the spectrum is smooth enough that the window folding operation merely appends a constant factor. Thus, for a gamma-ray (E, ℓ or M, ℓ) of yield Y, the spectrum of positron detector counts is

$$S_{\underset{(M)}{E\,\ell}}(B\rho) = 6.25 \times 10^{-4}\, Y\Omega p B\rho \;\Gamma_{\underset{(M)}{E\,\ell}}(p_+) \qquad (14)$$

since

$$\frac{dp_+}{dB\rho} = \frac{p_+}{B\rho} = 5.868 \times 10^{-4}$$

One possible weakness of the method arises from angular distribution difficulties. The spectrometer measures all yields at 20° with respect to its axis, so that (14) implicitly assumes

$$Y_{pair}(\text{total})/Y_{\gamma}(\text{total}) = Y_{pair}(20^{\circ})/Y_{\gamma}(20^{\circ})$$

It is comforting that for gamma energies as large as several times mc^2 such should indeed be the case. It is permissible to think of this as the effect of large (virtual) quantum momentum projecting the pair components predominantly in a forward direction. Quantitative results await the calculation of the positron angular distribution.

The assumption of plane waves for electron and positron should lead to a more accurate answer for this problem than for internal K-conversion, since both components are in continuum states. The Coulomb (second order) effect should contribute mainly to a redistribution of the positron spectrum toward the higher end, and the electron spectrum oppositely. Rose and Uhlenbeck[23] have estimated this for electric dipole and quadrupole radiation. Assuming the electron to be a spherical outgoing wave, they find, for the end point of the positron spectrum,

$$\begin{aligned} Q_{E1} &= \frac{2\pi}{137} Z\,(k^2+2)\left[k(k-2)\right]^{1/2}/k \\ Q_{E2} &= \frac{2\pi}{137} Z\,(3k^2+8)\left[k(k-2)\right]^{3/2}/3k^3 \end{aligned} \qquad (15)$$

Spectra computed from (12) are customarily corrected to match this ordinate, the ones for higher order spectra being scaled down proportionately. Only the upper 3 or 4 percent is affected.

An experimental suggestion as to the magnitude of this effect is gained by a comparison of the electron and positron spectra at the high energy end. This was performed for the pairs of the 3.57-Mev gamma-ray of Li^6, produced by the reaction $Be^9(p, \alpha)$, and appears in Figure 10. The upper half of the figure shows the electron spectrum, which consists mostly of Compton secondaries. The lower half shows the positron spectrum (dots) and the fraction of the electron spectrum judged to be pairs (crosses). The comparison is, of course, at the mercy of the Compton spectrum extrapolation; however this extrapolation is least arbitrary at the upper end, where most interest centers.

The difference between the two spectra is below the threshold set by experimental statistics. The apparent discrepancy at the high energy end is, however, suggestive of the effect of the Coulomb field and hints that its magnitude is comparable to that indicated by the end point formulas.

Another example of the art utilizes the 3.1-Mev line from $C^{12}(d, p)C^{13*}$. This measurement, previously performed by Thomas and Lauritsen, was repeated in order to gauge the advantage of using the scintillation-counter detector. The experiment was complicated by the presence of 10-minute positron-emitting N^{13} produced in a competing reaction. This affected the monitor readings primarily, since the detector bias excluded all annihilation radiation and most of the positrons (end point 1.2 Mev). At any rate, each run was followed by an equal counting period with no beam on target.

A 35 mg/cm^2 graphite flake was bombarded by 1.46-Mev deuterons, and the Compton spectrum produced in 0.7 g/cm^2 aluminum was measured; each point represented 14.4 microcoulombs. The positron spectrum from a 12.4 mg/cm^2 graphite flake was measured (55 microcoulombs per point), and it appears (4 percent time-dependent background subtracted) in Figure 5. The solid curves are theoretical spectra (Equations (12) and (14)), for electric dipole and quadrupole transitions, based on $Y\Omega$ evaluated from the Compton spectrum. The counts-to-background ratio was increased by a factor 5/3 over the Geiger counter work.

The excellence of the fit to the electric dipole curve speaks for itself. The two branches of the theoretical curve are the Born approximation (12) and a refinement suggested by the end point correction (15). Folding with the spectrometer window would add a small tail above the end point and decrease the spectrum slightly in the region of large curvature. That is, it would cancel a part of the end-point correction. Figure 5 therefore suggests that the end-point correction need not be made.

The reaction yield was 27 percent below Thomas' value for E_d = 1.46 Mev. This might have resulted from a small discrepancy in the bombarding energies, there being a resonance for $C^{12}(d,p)$ at 1.44 Mev[24]. This factor did not affect the internal pair conversion coefficient measurement.

II. RADIATION FROM Be^9+p

A. BACKGROUND

The 3.57-Mev gamma-ray produced by the proton bombardment of beryllium was first reported by Hushley[25], who found a resonance at 2.56 Mev bombarding energy, for gamma-rays and neutrons. Day and Walker[26] made the first accurate measurement of its energy, 3.58 ± 0.04 Mev, using a NaI(Tl) scintillation counter. They verified Hushley's suggestion that it followed the reaction $Be^9(p, \alpha)Li^{6*}$ by $\alpha - \gamma$ coincidences, improved the figure for the resonance energy (to 2.565 ± 0.005 Mev), and found the level width to be 39 ± 2 kev. They measured the thick target yield at 2.72 Mev as 4.76×10^{-6} gamma-quanta per proton ($\pm$ 10-15 percent). They found no other gamma-rays, and estimated the relative strength of any lower-energy line to be less than two percent, that of any higher-energy line to be less than one-half percent. Soon after the appearance of their paper, Hahn *et al.*[27] reported gamma radiation of energy greater than 6 Mev resonant at 2.56 Mev, apparently much less intense than the 3.57-line.

Above 1.53 Mev, Li^6 is unstable to decay into an alpha particle and a deuteron. Thus, the existence of a 3.57-Mev gamma-ray of great intensity is remarkable. Professor W. A. Fowler has pointed out, however, that it can be easily understood if the emitting level has spin zero, even parity. For this assignment, the α-deuteron decay cannot conserve both angular momentum and parity, and only gamma-emission can occur. The ground state is known to have spin 1[29], so the gamma radiation should be magnetic dipole if the above analysis is correct.

B. GAMMA RADIATION, 3.57 Mev

Various spectra of secondary electrons from the 3.57-Mev gamma-ray were observed in the beta-spectrometer. The main purpose was to measure the internal pair coefficient, but it was convenient also to make yield and energy measurements, using the techniques described in the preceding sections. The target employed throughout was a 19 mg/cm^2 Be foil.

Figure 6 shows the photoelectron spectrum from a 23 mg/cm^2 thorium converter, separated from the target by 0.050" Al. The gamma-ray energy measured from the mean momentum value of several such peaks is 3.574 $\pm$ 0.020 Mev. This includes a 6.5-kev converter shift[1]. Comparison of the thin converter Compton spectrum with that from the 3.097-Mev gamma-ray of $C^{12}(d,p)C^{13}$ (IV, B) gave an independent value 3.570 $\pm$ 0.015 Mev. The average is 3.572 $\pm$ 0.012 Mev.

The maximum possible Doppler shift is 26 kev, but the particle-group measurements are not available to indicate just how much should be applied. The expected lifetime, around 10^{-15} second, is sufficiently shorter than the stopping time, about 4 x 10^{-13} second, to suggest that the correction should be made. Thus, comparison of the particle values with 3.548 Mev will provide information on the lifetime of the state. Recoil from the low-energy alpha-particles produced is not sufficient to cause measurable Doppler broadening.

The "infinitely-thick" converter Compton spectrum for a bombarding energy of 2.665 Mev appears in Figure 7. The solid curve is the theoretical spectrum (Equation 8) for $Y = 4.27 \times 10^{-6}$ gammas per proton. The descent of the experimental points below 11.2 kilogauss-cm reflects the actual thickness of the aluminum converter - 350 mg/cm^2.

Comparison was made between this yield value and that computed from the area under the photo-peak (Equation 10) to find a point on the $\langle \sec\theta \rangle$ curve (Figure 4) used in that measurement.

The variation of the alpha-particle width with bombarding energy dictates that there be no level plateau on the thick-target yield curve. Accordingly, it was decided to calibrate the magnetic analyzer on this 2.565-Mev resonance in order to make a meaningful yield comparison with Day and Walker(27). Ordinarily, a beta-spectrometer is a fairly cumbersome instrument for such a task. At any rate, a detailed excitation curve was measured, the spectrometer being held at a constant current setting corresponding to the broad peak of the Compton distribution. This setting was checked continuously, during the measurement. In retrospect, slightly better results might have been obtained had several points on the Compton curve been taken at each bombarding energy. The field in the magnetic analyzer was measured with a null-reading fluxmeter. The zero of this device was checked at short time intervals to limit the energy drift of the beam to a few kev.

The resulting excitation curve is shown in Figure 8. Superposed is a "thin-target" curve obtained by differentiating the smooth curve which best fit the experimental points. The calibration is based upon this peak falling at 2.565 Mev. The width of the resonance was found to be 53 kev, which does not agree with Day's figure 39 kev. This is regarded as an indication of the perils of differentiating an experimental curve. At any rate, the yield at 2.72-Mev is 4.63×10^{-6} gamma-rays per proton, to be compared with Day's 4.76. It comes as a pleasant surprise that a scintillation counter is capable of such accuracy even with the optimum conditions provided by this experiment.

C. INTERNAL PAIRS

The positron spectrum was studied with particular care at the high-energy end and with progressively poorer statistics down to 0.65 Mev. The precision was limited by the background of scattered electrons and neutrons. To make full use of the scintillation counter detector and discriminator, the spectrum was studied in segments of about 20 percent, the bias setting in each case being such as to count all particles of energy greater than that corresponding to the lower end of the segment. For such a setting, no particles with less than half that energy would be counted. An idea of the background problem presented and the adjustments necessary is indicated by the fact that when the discriminator was set to count all particles of energy greater than E, the background, in counts per microcoulomb, was, to a few percent,

$$S(E, \text{Mev}) = 9 \left[\log (7/E)\right]^2 /4$$

at 2.63 Mev bombarding energy.

A generous overlap between measured segments was taken and the background adjusted for a best average fit. It was interesting that in every case the adjustment was equal to the difference in zero-lens-current background, within statistics.

Because of the sloping yield curve, the magnetic analyzer setting was checked frequently during the measurement. As a further assurance against drift, the Compton spectrum (thick converter) was measured before and after the positron run.

The resulting spectrum for $E_p = 2.63$ Mev is shown in Figure 9. The scale of the theoretical curves (12), (14) is determined by the yield value 3.94×10^{-6} γ/p. The asymmetry of the spectrum is caused by the momentum-proportional spectrometer window. As with the $C^{12}(d,p)C^{13*}$, 3.1-Mev pairs, the experimental data suggests that the end point correction (15) be omitted.

The curve most closely followed by the experimental points corresponds to magnetic dipole (M1) radiation. Electric quadrupole (E2) radiation cannot definitely be excluded, but a reduction of 18 percent would be required to match the electric octopole (E3) curve in the region above 8 kilogauss-cm, which is outside the estimated experimental error. Electric dipole is definitely excluded, as is magnetic quadrupole and higher multipoles.

A sharper distinction can be drawn between the several multipoles by computing a total internal-pair conversion coefficient from the experimental spectrum. This was done by computing the area under the jagged curve formed by joining adjacent points with straight lines from 3.5 kg-cm to the end point and comparing with areas under corresponding portions of the theoretical curves. The area under the Ml curve fell 4.4 percent below the experimental curve, that under the E2 curve 13 percent above it. On the basis of the internal pairs alone, therefore, E2 radiation is unlikely but cannot be excluded with certainty.

One might argue with some justice that the internal pair coefficients depend upon the areas under curves from which the spectrometer-window fold has been removed rather than those of Figure 9, and that therefore unfolded curves should be compared in finding the multipolarity of the gamma-ray. The reply is that such a procedure magnifies the role of the low-energy points, for which statistics are much poorer, and that the present figures reflect more accurately the true relationship between data and theory. Incidentally, the suggested computation finds the Ml curve 3.5 percent below experiment and the E2 curve 15 percent above.

A comparison of electron and positron spectra was made to check the validity of the Born approximation in the theoretical analysis. This appears in Figure 10 and has been discussed in (I, E). In the lower half of the figure, dots represent positrons, crosses represent electrons, minus assumed Compton spectrum. The match is quite good.

D. CAPTURE RADIATION

The results of Hahn *et al.*[27] prompted a search for the high energy radiation resonant at this bombarding energy. A 690-mg/cm^2 Al converter was attached to the Be foil used in the previous experiment, the bias was set at 6.4 Mev, and the spectrum was surveyed.

An extremely weak Compton spectrum was found, produced by a gamma-ray of energy 8.1 $\pm$ 0.2 Mev. The yield was 3×10^{-9} gammas per proton at 2.59 Mev, or 1000 times less than the 3.57-Mev line. The spectrum appears in Figure 12.

Time did not permit a simple check that this radiation was indeed resonant at 2.56-Mev, but its energy suggests that it probably is, and further that it results from a transition from the 8.89-Mev state of B^{10} to the 0.72 state.

In spite of the poor statistics (the rise 20 percent below the end point was less than a hundred counts for a 55-microcoulomb bombardment) the departure from the theoretical Compton spectral curve is enough to suggest that two lines are actually present. The second line is undoubtedly the well-known capture radiation to the ground state produced at the 998-kev resonance[29], and the spectrum has been drawn to match the known energy (7.4 Mev) of that line. (Its apparent yield is far below that quoted by Reference 29.) Note that there are no known resonances[14] other than the one at 2.56 Mev from which the 8.1-Mev line could originate. Further experiments on this line are anticipated, including a search for the 720-kev line presumed to be in cascade with it.

E. DISCUSSION

It was mentioned above that the forbidden α-d decay of the 3.57-Mev state would follow from the level's having zero spin, even parity. The internal pair spectrum presented here is unequivocal in assigning even parity to it (neither Ml nor E2 radiation involves a parity change) and, with somewhat less assurance, indicates that the radiation is magnetic dipole, supporting the J = 0, even, assignment.

Such support is not altogether superfluous, because an alternative hypothesis exists regarding the particle stability of the level. To the extent that nuclear forces are charge independent, a nuclear state is characterized by an isotopic spin quantum number (T) which will be conserved in nuclear reactions. Thus, if the 3.57-Mev state has T=1, it cannot decay into an alpha and a deuteron, each with T=0. (For an introduction to the lore of isotopic spin, see E. P. Wigner[30]; see R. K. Adair[31] for a discussion of its implications in nuclear reactions.) The extent to which the decay is inhibited is determined by the purity of the state.

Actually both J = 0, even, and T = 1 are now believed to be true. The 3.57-Mev level lies very near the anticipated location of the analogue of the He^6 and Be^6 ground states (J = 0, even, presumed). This mass-6 triad (and in particular, the last mentioned fact) forms a strong argument for the near charge-independence of nuclear forces. Charge symmetry alone would imply the existence of the analogue level but would not determine its position.

Note that T = 1 for the 3.57-Mev level implies T = 1 for the 8.89-Mev level of B^{10} from which it proceeds. The significance of the assignment might well be questioned where such a highly excited level is involved. In this connection it has been remarked that the ground and first-excited (2.18-Mev) states of Li^6 (T = 0) do not show this resonance, which would follow from T = 1 for the 8.89-Mev level. Unfortunately, for the Li^6 ground state (J = 1, even), it would as readily follow from the 8.89-Mev level's having J = 0, even. This assignment would likewise forbid the 2.18-Mev state's showing resonance if it has odd spin, even parity or vice-versa. Recent He^4+d scattering experiments by T. Huus and T. Lauritsen (in Copenhagen) indicate that the 2.18-Mev level has J = 3, even (preliminary results, unpublished). Furthermore, the 8.89-Mev level must have even spin, even parity, or odd spin, odd parity, in order to produce the 3.57-Mev level; and zero, even, is a likely choice on the basis of the cross-section for the (p, α) reaction. Thus it may be that another opportunity to observe isotopic-spin selection rules in action is subverted by the operation of ordinary angular momentum and parity selection rules.

APPENDIX. THIN CONVERTER COMPTON SPECTRUM

This section contains an account of certain problems arising in the evaluation of experimental data and has little bearing on the main body of II.

Figure 11 shows the Compton electron spectrum produced in a 23 mg/cm^2 Be foil. This curve proves useful in the analysis of other reactions (see $C^{12}(d,p)C^{13*}$, IV, B) and provides an energy measurement independent of the photopeak data.

An attempt to fit the observed spectrum with a theoretical one was unsuccessful. The dotted curve is the plot of Equation (1) with a numerical fold of the 1.9 percent window and a Landau-Thomas energy loss distribution function for a converter of thickness 23 x (sec 20^o) mg/cm^2. (20^o is the spectrometer acceptance angle.) The scale was set to match the peaks. The accurate (momentum dependent) value of $\langle \sec \theta \rangle$ was used in (1), although the correction was less than 2.5 percent maximum. The energy-loss distribution fold shifted the peak of the spectrum 22 kev, about 0.9 times the most probable energy loss, but contributed almost no broadening. The same difficulty was encountered by Rasmussen(1), who used an assumed loss-distribution and found it necessary to assume a spectrometer window 1.2 times his measured one. He ascribed this to a large gamma-source size resulting from imperfect localization of the incident beam. The discrepancy in the present case is not believed to be the result of such a phenomenon.

Actually, a large portion of the discrepancy in Figure 11 must be attributed to the breakdown of the approximations of the

Landau theory of energy losses. The contribution to the spectrum from the surface layers of the converter cannot be neglected as it can in a thick-converter yield measurement. In fact, the mean-free path for single scattering is of the order of 3 mg/cm^2 which is more than 10 percent of the total converter thickness used. An adjustment for this should eliminate the discrepancy on the high energy side.

Multiple scattering certainly contributes to the low energy discrepancy, and may explain it entirely.

It is appropriate, before leaving the subject, to mention another unsolved, and perhaps related, problem. Thick converter Compton data produce gamma-ray energy values which are almost uniformly 0.6 percent too high. This can be seen in the $C^{12}(d,p)C^{13*}$ data of Thomas and Lauritsen and is mentioned by Rasmussen (Thesis p. 82). Figure 7 gives an energy value 3.596 Mev for the Li^6 gamma-ray under scrutiny, 22 kev (0.62 percent) above the accepted photopeak value. This is outside the expected limit of internal consistency. The same result obtained for five other gamma-rays reported here - the only ones for which a check could be made.

This phenomenon is independent of the resolution width assumed and probably arises from distortions of the energy loss spectrum suggested by the thin converter data.

It is interesting, but perhaps coincidental, that the peak-match shown in Figure 11 results in a gamma-ray energy within 5 kev of the photopeak value. Matching extrapolated edges produces a 23-kev error. Matching a theoretical peak broadened by folding with an oversize window would produce a comparable error.

III. RADIATION FROM $Be^9 + d$

A. BACKGROUND

The first excited state of Be^{10}, at 3.37 Mev, has been studied by means of the reaction $Be^9(d,p)\,Be^{10*}$. In particular, the angular distribution of the proton group from this reaction has been measured at bombarding energies up to 14.5 Mev[14]. The most convincing work was that of Fulbright et al.[32] who bombarded at 3.6 Mev but extended their observation of the distribution to smaller angles than had been studied by previous investigators. Their analysis by the Butler stripping theory[33] showed that both the ground state and the 3.37-Mev state are formed by the capture of a neutron of $\ell = 1$. Both levels, then, have even parity and spin ≤ 3. The ground state is presumed to have J = 0, and the angular correlation of short range protons and 3.37-Mev gamma-rays is consistent with J = 2 for the excited state[34].

The above evidence suggests that the 3.37-Mev gamma-radiation is electric quadrupole (E2). The spectrum of internal pairs was studied by Thomas and Lauritsen[3], but a high background and the presence of a 3.6-Mev gamma-ray from $Be^9(d,n)B^{10*}$ conspired to make their results inconclusive. The use of discrimination in the detector unit offered hope that the background uncertainties might be reduced, and it was therefore decided that a second measurement be made.

Earlier studies of the gamma radiation from $Be^9 + d$[35] were made at bombarding energies below 1.6 Mev. A corollary to the remeasurement of the pair spectrum, then, was a survey of the radiation produced at higher bombarding energies.

B. 3.60- AND 3.37-MEV GAMMA-RAYS; COMPTON SPECTRUM

A beryllium target 19 mg/cm^2 thick was bombarded by 2.5-Mev deuterons. The monitor counter was surrounded with a two-inch thickness of boron-loaded paraffin in addition to the usual lead shielding in order to count only gamma-radiation from the target. In addition, extra shielding was placed between the beam-defining slits and the spectrometer as it was found that the scatter of detector counts was increased when beam regulation became erratic. Each of these measures produced a net improvement in the results. The monitor counting-efficiency was checked with a standard Co^{60} source before and after each day's run and showed no variation. It was thus possible to check that current measurements did not change when going from Compton to positron spectrum.

The Compton spectrum produced in a 350 mg/cm^2 Al converter is shown in Figure 13. The counts-to-background ratio was 30 percent worse than Thomas' for two reasons: a large fraction of the background consisted of high-energy neutron counts; also, the higher bombarding energy produced relatively more high-energy reaction gamma-rays whose Compton electrons added 70 percent to the existing background. In the positron spectrum, where the former effect predominated, the stilbene excelled the Geiger counter by 10 percent.

In spite of this, the present results bettered the earlier ones significantly. The seven-fold greater yield at the higher bombarding energy improved the positron statistics; the higher electron background was still negligible; and the gamma-ray yield could be found with less chance for error.

The last named circumstance arose from the possession of an excellent experimental Compton spectrum measured with identical geometry and having almost the same energy as the higher energy line: the spectrum of the 3.57-Mev line from $Be^9(p,\alpha)Li^{6*}$ (Figure 7). Thus, the extrapolation of the 3.60-Mev spectrum in Figure 13 is based on experimental data rather than a theoretical formula - which could not be trusted below 11.7 kg-cm. The success of this procedure is indicated by the overall agreement between the experimental points and the theoretical spectrum of the 3.37-Mev line drawn above the extrapolated 3.60-Mev curve.

Use of the 3.57-Mev spectrum provided an accurate energy measurement, also. Comparison of the curves shows that the two deuteron-produced lines differ from the original by +23 kev ($\pm$8) and -221 kev ($\pm$25) respectively. The Li^6 line is at 3.572 $\pm$ 0.012 Mev (II, B); the resulting energies and earlier values (from photopeaks, E_d = 1.2 Mev), are given in Table I. Yields computed from (8) are included. It is worth noting that direct energy determinations from the Compton end points produce values 0.6 percent high (see II, Appendix).

Doppler shift corrections have not been made; the current data should have up to 9 kev more Doppler shift than that with which it is compared. The predominantly backward (CM) distribution of the residual nuclei, characteristic of the stripping process, probably suppresses any Doppler effect by about 50 percent, however. This estimate is based on Fulbright's[32] measured angular distribution of protons from $Be^9(d,p)Be^{10*}$.

TABLE I

Gamma-Ray Energy (kev) This experiment	Gamma-Ray Energy (kev) Reference (35c)	Level Position from Particle Groups	Yield, E_d=2.5 Mev (10^{-6} γ/d)
3595 ± 14	3604 ± 30	3530 ± 60[36]	5.7 ± 0.7
3351 ± 27	3380 ± 15	3372 ± 13[37]	20.4 ± 2.0

C. 3.37-MEV GAMMA-RAY; INTERNAL PAIRS

The same target was used in both positron and Compton electron measurements. The precautions to insure consistent current measurement were described in the previous section. The presence of a line at 2.87 Mev limited the amount of the spectrum which could be studied. Figure 14 contains the results of the best run performed and the theoretical curves (12), (14) based on the measured yields. The flat background is well substantiated by considerable data from different runs not shown.

The points of the 3.60-Mev positrons fall 30 percent below the electric dipole (El) curve. This is sufficient to exclude El, even allowing double the statistical error in the assumed background level, but little more can be said. For the purpose of providing a background for the 3.37-Mev positrons, the 3.60-Mev transition was taken as Ml. This choice is discussed in the next section.

Most points represent a 14.4 microcoulomb bombardment; some represent twice that amount, as is indicated by the rms deviation shown.

The data on the 3.37-Mev line below 8.5 kg-cm can be characterized as follows: the deviations of the several theoretical curves from the experimental one are E1, +31 percent; E2, -11 percent; and M1, -21 percent. Expressed somewhat differently, to force an agreement with E1, the yield would have to be lowered 26 percent; to force an agreement with M1 it would have to be raised 26 percent. The 3-37-Mev transition appears therefore to be E2, and the first excited state of Be^{10} has J = 2, even.

Note that a part of the disagreement above 8.5 kg-cm may be attributed to a 20-kev error in the measured gamma-ray energy.

D. DISCUSSION

A Butler analysis of the neutron angular distribution from $Be^9(d,n)B^{10*}$ shows the 3.58-Mev state to be formed by the capture of protons with $\ell = 1$[36]. The parity of the state is therefore even and the spin is $\leqslant 3$. The level decays to both the ground state (J = 3, even) and the 0.72-Mev state (J probably 1, even), the latter transition being 2.7 times as frequent[35e]. This strongly suggests spin 1 or 2, with 2 somewhat more likely (Richards[38]). This choice indicates magnetic dipole transitions for both branches. It is worth pointing out that a spin 1 assignment is not entirely unreasonable. This would make the higher energy transition E2, but it has been shown by Goldhaber and Sunyar[39] that E2 lifetimes are occasionally much shorter than indicated by single-particle model formulas. Such an assignment would only improve the agreement between the E2 curve and the experimental points of the 3.37-Mev line and would not change the conclusions of the experiment.

The (J = 2, even) assignment for the 3.37-Mev state of Be^{10} confirms the suggestions of the previous particle distribution[32] and correlation[34] experiments. A careful search by Ajzenberg[36] failed to reveal any states of lower excitation. Be^{10}, then, is the fifty-fifth even-even nucleus believed to have J = 2, even, for its first excited state[40]. Two are known which have J = 0, even, and a few exist for which spin 1 has not been finally excluded.

The 1.74-Mev state of B^{10} is fairly certain to be the analogue of the Be^{10} ground state. In B^{10}, then, a state with J = 2, even; T = 1, should appear at about 1.74 + 3.37 = 5.1 Mev. The attempts to find it are interesting. (Be^9 + d) slow-neutron threshold data of Bonner and Butler[41] reveal levels at 5.11 Mev and 5.17 Mev. Ajzenberg's[36] angular distribution of a neutron group going to 5.14 Mev connotes odd parity, but this could represent both levels or one dominant level.

Jones and Wilkinson (in press) have studied the reaction $Li^6(\alpha,\gamma)B^{10}$. They find only the upper member of the doublet, at 5.162 ± 0.008 Mev, with a radiation width $\omega\Gamma = 0.2$ev. The lower member has $\omega\Gamma < 0.004$ ev. As is usual with isotopic spin experiments, the results are somewhat ambiguous, even though it seems clear that one of the levels does have T = 1. The obvious suggestion is that the lower level has T = 1 and is therefore suppressed, because T = 0 for Li^6 and He^4. This is unsatisfactory, since Radicatti[42] has shown that the Coulomb perturbation introduces a 0.25 percent intensity of T = 1 in the Li^6 ground state and thereby reduces considerably the discrimination against the formation of a T = 1 state in the compound nucleus. Accordingly, Jones and Wilkinson suggest that perhaps the upper state has T = 1 but the lower state has J = 2, odd, and that its diminutive width results from the isotopic spin selection rule on electric dipole transitions: no T = 0 to T = 0. Measurements discussed in the following section have some bearing on this question.

E. HIGH ENERGY RADIATION

Chao et al.(35d), bombarding Be at 1.5 Mev, measured thick-converter Compton spectra of gamma-rays with energies (in Mev): 3.97 ± 0.08, 4.47 ± 0.07, and 5.2 ± 0.1. At $E_d = 3.0$ Mev, Meyerhof et al.(43) observed 6.0- and 6.7-Mev gamma-rays.

The region above 3.6 Mev was surveyed at $E_d = 2.5$ Mev, using a thick converter (700 mg/cm^2 Al). The primary purpose was to find lines strong enough for internal pair measurements; in this the experiment was unsuccessful. Two lines dominated the spectrum, the 4.4-Mev line and one at 6 Mev. These were studied in some detail, neither having been assigned previously to a definite transition. The spectra appear in Figures 15 and 16. Each point represents 14.4 microcoulombs of deuterons.

The end-point measurement of the lower-energy line gave $4.462(1-0.006) = 4.435 \pm 0.03$ Mev; the yield was 0.99×10^{-6} γ/d. Comparison with the Compton spectrum of the 3.57-Mev line of Be^9+p, showed the energy difference to be 866 ± 20 kev. This gives for the energy of the line 4.44 ± 0.03 Mev, in excellent agreement.

The addition of 4.44 ± 0.03 and 0.72 ± 0.00 gives 5.16 ± 0.03. A 20- to 40-kev Doppler shift, which depends on the angular distribution of residual nuclei, robs this datum of its apparent significance. The initial state must remain unassigned, but the lower member of the doublet seems the more likely choice. This assignment and the low intensity of 5.2-Mev radiation[35d], would confirm Ajzenberg's findings and bear favorably upon Wilkinson's suggestion.

The 6.0-Mev gamma-ray presented a problem of a different sort: that of assigning an emitting nucleus. A level is believed to exist in the region of 6.2 Mev in Be^{10} [14]. B^{10}, on the other hand, has levels at 5.93 $\pm$ 0.02 and 6.12 $\pm$ 0.04 [14]. The gamma-ray energy, from the end point is 6.013(1-0.006) = 5.98 $\pm$ 0.04. A Doppler shift of 50 kev is possible, therefore assignment to the 5.93-Mev level would seem reasonable. 1.6×10^{-6} γ/d is the yield at 2.5 Mev. Any gamma-ray in the 400-kev interval above this line has an intensity less than 10 percent of that figure. Over the next 1-Mev interval the upper limit is 2 percent.

This result left unexplained the radiation from the 6.2-Mev state presumed to exist in Be^{10}. To get an energy check, (and insure that the line is single) the thin converter Compton spectrum was measured. To the 23 mg/cm^2 Be target was added 34 mg/cm^2 of Al, forming a target about a half-resolution width thick. The inset in Figure 16 shows the result, with the same units as the complete scales. A comparison was made with the 6.110 line from C^{13}+d (not shown). The target was 17 mg/cm^2 C plus 23 mg/cm^2 Cu, and bombarding energy was 1.45 Mev. The best curve match gave an energy difference of 116 $\pm$ 20 kev (poor statistics produced by a high background caused most of the uncertainty). This gives for the energy 6.110-0.116 = 5.99 $\pm$ 0.04 Mev, which confirms but does not improve upon the initial measurement. Finally, an excitation function near threshold was attempted in hopes that this might confirm the assignment. The thick-converter Compton spectrum was not sufficiently sharp to be easily detected, and the thin-converter spectrum was too weak. Accordingly, a NaI scintillation spectrometer with 10-channel differential discriminator was employed in place of the beta-spectrometer. This arrangement resulted from the courtesy of H. H. Woodbury, who was most helpful throughout.

The counter was set up with crystal about 2 cm from target along a line perpendicular to the beam. Resolution was found to be 7.3 percent. A 0.070 mg/cm^2 (5.25-kev) Be foil (supplied by Dr. Hugh Bradner) was the target, backed with 0.005" tantalum, and oriented at 45^o with respect to the incident beam. The 2.62-Mev gamma-ray from ThC" was used to calibrate the discriminator. The double line resulting from pair production in the crystal with escape of one or both annihilation quanta was studied. The gamma-ray energy was measured as 5.93 Mev.

The experiment was not successful in that the presence of a resonance just above the threshold (the broad 2.1-Mev peak previously identified by long range protons[14]) prevented any conclusion as to the characteristic shape of the curve at threshold.

The lowest bombarding energy for which a peak was definitely seen was 1.95 Mev. The threshold for a 5.93-Mev gamma-ray (with Doppler shift) is 1.92 Mev in B^{10}, 1.64 Mev in Be^{10}. The Coulomb barrier is adequate to produce a 300-kev uncertainty in the threshold of a (d,p) reaction, so the datum is not meaningful.

The gamma-ray may tentatively be assigned to the 5.93-Mev level. The only basis for this is the excellent energy agreement, which is unique to this level.

The gamma-ray appears to exhibit a Doppler shift. It is emitted in competition with the Li^6 - α decay. These data suggest a high spin value, probably 3 or 4.

IV. RADIATION FROM C^{12} + d

A. BACKGROUND

A controversial level in C^{13} which had hovered around 3.8 Mev for many years was shown to be a doublet by Rotblat(44) in 1950. He used photoplates to measure proton groups from the reaction $C^{12}(d,p)C^{13*}$, produced by 8-Mev deuterons, and found the level excitations to be 3.683 and 3.884 Mev. A gamma-ray at 3.65 $\pm$ 0.05 Mev following C^{12} + d was reported by Meyerhof (priv. comm. to Fay Ajzenberg), who used a scintillation spectrometer. Thermal neutron capture by C^{12} produced one at 3.68 $\pm$ 0.05 Mev. Bartholomew and Kinsey(45), who measured it with a pair spectrometer, reported its intensity to be 0.3 photon per capture and that of any 3.9-Mev line to be less than 0.06 photon per capture. A more elucidative gamma-ray study of C^{12} + d was felt to be possible.

B. COMPTON SPECTRUM

A 40-mg/cm^2 graphite flake was used as target and Compton converter. A Geiger telescope monitor was used and was adjusted to be insensitive to the annihilation quanta produced by decaying N^{13}. The detector bias was set well above the maximum positron energy, and the search for high-energy radiation was thus free from the customary uncertain background usually attributed to circulating N^{13} gas. Even so, cooling-off periods were necessary in order that the annihilation radiation should not overly raise the singles rates in the monitor components.

The spectrum observed at deuteron energy 2.4 Mev is shown in Figure 17. Each point represents bombardment by 55 microcoulombs. The flat background is extrapolated from points measured above 14 kg-cm, not shown. The presence of two gamma-lines is evident, but the detailed analysis of the data requires extra information. That is, it is not possible to sketch in the line shapes shown, using only the experimental curve, without ambiguity.

One solution to the problem utilized the Compton spectrum of the 3.1-Mev line produced in the same converter. The best curve through the experimental points was (vertically) scaled to match the spectrum of Figure 17 in the region of 13.5 kg-cm, making a small allowance for the change in spectrometer window. The peak of the curve was traced in and the 3.1-Mev spectrum discarded. The remainder of the high-energy spectrum was then defined by requiring that the second curve be an exact multiple of the first, comparing points equal distances below the respective end-points.

The first attempt produced a spectrum with an abrupt level portion about 6 percent below the peak. This was eliminated when it was realized that a 3.4-Mev gamma-ray from C^{13} (1 percent) + d would produce a rise in this region. The contribution was estimated from a run using an enriched (50 percent)C^{13} target; it is indicated by the dashed line in Figure 17. When this was subtracted, the resulting curve agreed well with the 3.1-Mev spectrum. At a later time, the Compton spectrum of the 3.57-Mev line of $Be^9(p,\alpha)Li^{6*}$ was measured, using a Be target-converter 23 mg/cm^2 thick. (See Section II, Part D, and especially Figure 11). The agreement with the curves of Figure 17 was remarkably good and imparts much confidence in the technique.

In the course of the C^{13}+d measurements, it was established that neither of the new gamma-rays was produced in such a reaction.

Another approach to the extrapolation problem was tried as a further check. The spectrum was measured at E_d = 2.07 Mev, where the relative yield of the two lines was drastically different. The previous curve (background subtracted) was scaled to match the new one over the region above 13.5 kg-cm and subtracted from it. As is shown in Figure 18, the exact line shape was not preserved, but the end-point and the peak were reproduced unshifted. The relatively greater yield of the 3.4-Mev line at the lower bombarding energy is in evidence.

Point-to-point comparison of the thin-converter Compton spectra of the 3.1- and 3.57-Mev lines produced an accurate figure for the energy difference between the two gamma-rays, 469 $\pm$ 14 kev (taking account of a 17 $\pm$ 10 kev difference in Compton converter shifts). The use of Thomas and Lauritsen's[3] value for the energy of the lower line, 3097 $\pm$ 5 kev (+ 4 $\pm$ 2 kev extra Doppler shift), gave for the Li^6 line a new energy value, 3570 $\pm$ 15 kev, independent of the photopeak data. The average of these two values was taken as a best value 3572 $\pm$ 12 kev.

A careful comparison was then made between these two spectra and those of the new carbon lines. The resulting energies of the new lines are 3684 $\pm$ 20 and 3843 $\pm$ 14 kev, and their energy difference is 160 $\pm$ 15 kev.

Particle-group measurements of the level energies (in kev) are:

C^{12}(d,p), 3683 and 3884, Rotblat[44] (photoplate); C^{12}(d,p), 3686 ± 11, Van Patter et al.[46] (magnetic spectrometer); C^{12}(d,p), 3680 ± 30 and 3850 ± 30, Bockelman et al.[48]; N^{15}(d,α), 3677 ± 5, Malm and Buechner[47], (magnetic spectrometer). The only disagreement with the gamma-ray data is Rotblat's value for the upper level 3.884 kev. He does not state a probable error. It is interesting that little or no Doppler shift seems to be indicated for the low energy line; this will be discussed later.

Thick converter Compton spectra were measured in the course of the study of the internal pairs; these appear in Figure 19 (700 mg/cm^2 Al converter). The gamma-ray yields at E_d = 2.4 Mev are:

3.84-Mev line	4.3 x 10^{-6} γ-quanta per deuteron
3.68-Mev line	5.8 x 10^{-6} γ-quanta per deuteron
3.10-Mev line	62 x 10^{-6} γ-quanta per deuteron

The quality of the fit between experimental and theoretical spectra is suggested by the energy values (corrected) determined from this measurement, viz., 3677 and 3838 kev.

An excitation curve (see Part D), Figure 22, gives the yields at other energies. At E_d = 8 Mev, the upper line is 9 times as intense as the lower one[44c].

A search for higher energy radiation from C^{12} + d at E_d = 2.7 Mev was unsuccessful. Because of the large background from C^{13} (1 percent) reaction gamma-rays, an upper limit on intensity was uncertain. A survey of the spectrum (at 2.2 Mev) produced the following lines too energetic to be produced by C^{12}(d,p/n): 6.1-Mev, Y = 0.25 x 10^{-6} γ/d; 6.7-Mev, Y = 0.044 x 10^{-6} γ/d; and 8.56-Mev,

$Y = 0.0233 \times 10^{-6}$ γ/d. The first two lines are produced by C^{13} + d, and further measurements on them will be reported in a separate publication.

The last line probably follows secondary (fast) neutron capture in the 700 mg/cm^2 Al converter. It does not appear when a copper converter is employed. This would not be the first instance of such an occurrence. A search for delayed radiation produced by deuterons on a 0.040" Be disk once revealed a beta-spectrum with a half-life of the order of a second and an end point at 3.5 Mev. This was attributed to He^6, produced by the reaction $Be^9(n, \alpha)He^6$. It disappeared when a foil of one-tenth the thickness was substituted.

C. PHOTOELECTRON SPECTRUM; 168-KEV GAMMA-RAY

Assuming tentatively that the 3.84-Mev line was produced by a transition in C^{13}, there was reason to believe that it was magnetic quadrupole. If so, lower-energy transitions of lower multipole order might successfully compete with it. Accordingly, the spectral region around 160 kev was surveyed.

The detector for this experiment was an Amperex 150-C Geiger counter with a 3.5 mg/cm^2 mica end-window. The high background of N^{13} counts could not be avoided, and alternate beam-on, beam-off count readings were necessary.

The spectrum of photoelectrons produced in a 3.4-mg/cm^2 Th foil is shown in Figure 20. There appear the K-, L-, and M-shell photopeaks of a gamma-ray whose energy is 168.2 ± 1 kev.

To each photopeak energy (computed from a momentum which included a 5.3 ± 1.2 g-cm earth's field correction) was added the atomic binding energy correction[7], the converter shift, and the target bias, 0.3 kev. The converter shifts were estimated by extrapolating the Christy-Cohen curves (given by Hornyak et al.[1]) and were little more than guesses; they were taken as 0.5 ± 0.3 kev for the K-electrons and 0.9 ± 0.4 kev for the L- and M-electrons. The K- and L-peak values for the gamma-energy agreed (fortuitously) to 0.1 kev; the M-peak, with poorer statistics, gave a one-kev higher answer. The lower value, quoted above, was the one adopted.

A noticeable feature of the photo-spectrum is the much-reduced K-peak amplitude, compared to those of the L- and M-peaks. Recent experimental investigations by K. Marty[49a] and Kai Siegbahn[49b] indicate that the well-known four-to-one K/(L + M) ratio is a fair approximation even at this low energy. The difference arises mostly from scattering effects. The converter and the counter window are each 3 1/2 mg/cm^2 thick, which is less than 3/4 transport mean free path for the L-electrons and nearly 3 transport mean free paths for the K-electrons. The "transport mean free path" is defined[1] as the distance in which the mean square scattering angle becomes $\frac{\pi}{4}$. It is approximately equivalent to the "scattering length" of Goudsmit and Saunderson[50]. No electrons with momentum less than 650 gauss-cm (35 kev) were counted, in fact. Their theoretical range in Al is 2.2 mg/cm^2, so this is not surprising. It is thought that these absorption effects did not appreciably shift the photo-peaks.

Several other difficulties prohibited an accurate yield measurement. A photo cross-section of 640 barns (atomic) was found by interpolating between empirical figures for lead and uranium[51]. In order to get sufficient counts for an accurate spectrum, the converter was placed only 0.005'' from the target, making the empirical $\langle \sec \theta \rangle$ curve (Figure 4) inapplicable. Estimates on $\langle \sec \theta \rangle$ of 2.1 (K) and 1.8 (L) were found by extrapolating empirical data of Thomas[3] to the energies involved. A peak was also measured with standard geometry and therefore poor statistics. The computed intensity agreed to 20 percent with the estimate.

The 168-kev line yield is about 2×10^{-6} γ/d at 2.4 Mev bombarding energy, or a little less than half of the weaker of the high energy lines. The intense background prevented the detection of the internal conversion peak.

A search was made for radiation which might correspond to a transition to the 3.1-Mev level. The scintillation-counter detector was employed. 2.5-Mev deuterons bombarded the 40 mg/cm^2 graphite flake, which was backed by 35 mg/cm^2 Al and 14 mg/cm^2 Th, and the spectrum was surveyed from E_γ = 530 to 1120 kev. It was necessary to take alternate beam-off background readings. The result appears in Figure 21. Dots represent prompt radiation, circles delayed. The delayed counts (normalized on counting time under near-equilibrium conditions) were included to show the L-photopeak of the annihilation radiation, which falls very near one of the anticipated lines, and which aids the imagination in analyzing the prompt spectrum. The apparent absence of a prompt photopeak places an upper limit on its yield at 0.2×10^{-6} gamma-quanta per deuteron, or about 3 percent of the ground state transitions from the 3.68- and 3.84-Mev levels.

D. EXCITATION FUNCTION; ASSIGNMENT OF THE RADIATION

A beta-spectrometer appears to be able to gather little more than circumstantial evidence regarding the transition involved for a measured gamma-ray. The only solution of this difficulty is the amassment of so much evidence of this sort that the conclusion will be accepted, as it were, by default. It was in this spirit that an excitation function, or relative yield curve, was measured for each of the lines under investigation. The one whose assignment needed bolstering was, of course, that at 168 kev, but little harm was done if it was made certain that no contradictions were entailed in associating the high energy lines with the C^{13} levels which matched their energies.

For the 3.68- and 3.84-Mev lines, the procedure was as follows. The individual Compton spectra, (at $E_d = 2.4$ Mev) shown in Figure 14, were regarded as prototypes, f(Bρ), g(Bρ). At each bombarding energy, 15 points were recorded, between 12 and 15 kg-cm. A background was drawn, and the remaining spectrum F(Bρ) was analyzed by a least-squares method to find the amplitudes of f and g relative to those at 2.4 Mev.

The same procedure was followed with the low-energy line. The prototypes f and g were the K-shell photopeak and a linear (measured) background beneath it, shown in Figure 20. Nine measurements were made at each analyzer setting, and time-dependent background was subtracted.

The analyzer was calibrated on the 1.757-Mev resonance in C^{13} +p, using a scintillation spectrometer to record gamma radiation.

The various excitation functions are plotted in Figure 22. Dots and plus-signs represent the 3.68- and 3.84-Mev lines, respectively; curves are drawn through these points. Their absolute yield is plotted. Crosses (x's) are the points for the 168-kev line, normalized to match the 3.84-Mev line at 2.4-Mev. The circles represent the background to the 168-kev photopeak. This background consists for the most part of low-energy Comptons from the 3.1-Mev line and may be taken as proportional to its yield. This curve is normalized to match that of the 3.68-Mev line at 2.4-Mev.

That the normalization was designed to display the similarities of the matched curves goes without saying. That the 168-kev excitation function will match only that of the 3.84-Mev line is likewise apparent, and this is the most important result of the measurement.

There are other features worth noting. The disagreement near the threshold may be a manifestation of the presence of the 3.9-Mev line of C^{13} (d,n). More likely, it is experimental error. The behavior of the 3.68-curve in the region below 1.9 Mev is indicative of resonance. Ground-state neutrons (to N^{13}) and 3.1-Mev gamma-rays show a broad (Γ = 200 kev) resonance at 1.73 Mev(24), and it would appear that this gamma-ray shows it also. The 3.84-Mev line is too weak at this point for the detection of any resonant character.

The 3.68- and 3.84-Mev gamma-rays may be assigned as ground-state transitions from the levels of those energies in C^{13} without further comment.

The evidence for regarding the 168-kev line as a transition between these levels is as follows:

1. No contradiction is involved.

   a. The energy balance is excellent.

   b. The excitation curves for the lines posited to originate with the 3.84-Mev level are identical, within statistics.

   c. The intensity of the 168-kev line is definitely less than that of the 3.68-Mev line.

2. There exist, as yet, no other energetically possible levels to which it can be assigned.

   a. $C^{12}(d,\alpha)B^{10*}$ is possible by a margin of less than 70 kev. The occurrence of this reaction would require an unreasonably large α-particle width; and no such level is known to exist in B^{10}.

   b. It was checked with a C^{13}-enriched target that the initial nucleus is C^{12}.

   c. To be assigned to N^{13}, the line would have to arise from a level below 1.3 Mev, and no such level has been observed.[14]

   d. A search for higher-energy radiation from C^{13*}, with which this line might compete, was unsuccessful. Such a level would have to lie below 4.3 Mev.

This assignment is therefore quite reasonable and will tentatively be assumed to be correct.

E. INTERNAL PAIRS

It will be shown in the next part (F) that the presence of the transition between the 3.84- and 3.68-Mev levels makes a very strong suggestion regarding their spins. An attempt to verify this suggestion by internal-pair determination of the gamma-ray multipole order was therefore made. The yield measurement made in conjunction with this was described in Part B.

The deuteron energy was 2.5 Mev, an unfortunate choice because of a resonance at just that point: a slight drift could cause a substantial variation in yield.

The positron spectrum appears in Figure 23. Each point represents 110 microcoulombs bombardment. The theoretical curves are scaled by the respective yield values and have been shifted an amount equal to the most probable energy loss in the 40-mg/cm^2 flake.

The 3.84-Mev line is definitely not electric dipole (El) and seems unlikely to fit either of the next two curves (E2 and Ml). E3 and M2, the next two, are equally good choices. There is reason to believe in the M2 assignment, so this curve has been extrapolated to serve as background for the other line.

Below 9.4 kg-cm, there is a contribution of positrons from the 3.39-Mev line, encountered in the thin-converter measurement. This addition has been estimated, using a yield value suggested by thin-converter Compton data, and assuming the radiation to be El. The crosses represent the experimental points with this subtracted.

The multipole order of the 3.68-Mev line is in evident doubt. Possible causes of this are: bombarding energy drift between positron and electron measurements; incorrect positron background assumed, i.e., M2 instead of E3 assignment for upper line; incorrect extrapolation of 3.84-Compton spectrum; external pairs (less than

3 percent); and systematic error in yield calculation. Note that the error in the theoretical spectrum depends not upon the error in the 3.68-yield alone, but also upon that in the 3.84-yield. In fact, any systematic yield errors will be additive, weighted by the respective values.

In order for the various curves to agree with the experimental points in the region of 8.8 kg-cm, the yield should be adjusted by:

E1	-17.5 °/o
E2	+17.5 °/o
M1	+33 °/o
E3	+63 °/o

There seems to be no choice between E1 and E2, with M1 much less likely. In view of the serious disagreement with all curves, however, it cannot be finally excluded.

F. DISCUSSION

Rotblat's work included a measurement of the angular distribution of each proton group[44c]. The conclusion of his Butler analysis was: the upper level is formed by the capture of a neutron with $\ell = 2$, producing J = 3/2 or 5/2, even; the lower level is formed by the capture of an $\ell = 1$ neutron, and J = 1/2 or 3/2, odd.

The present experiment has shown a 168-kev gamma-ray emanating from the upper level in competition with one which has 23 times its energy. From the theory of emission probabilities the lower energy radiation must be of lower multipole order in order to compete. The choice here, on the basis of Rotblat's assignments is:

E1 competing with M2 for spin assignments 5/2, even, and 3/2, odd

M2 competing with M2 for spin assignments 5/2, even, and 1/2, odd

E1 competing with E1 for spin assignments 3/2, even, and either.

The first choice is the only one which makes lifetimes comparable within a factor of 10^4 according to contemporary models. It would be remarkable indeed if even the crudest estimate was off by that factor, and the first choice is tentatively accepted. The spins of the states in question are therefore suggested as being 5/2, even, and 3/2, odd.

The internal pair data confirm the first assignment. They agree with either M2 or E3 radiation from the 3.84-Mev state, and either of these may result from a 5/2, even, to 1/2, odd, transition. They distinctly exclude electric dipole radiation, which is the only other choice allowed by the Rotblat spin assignments.

It would be expected offhand that the pair data would have no bearing on the spin of the second state. For either possible assignment, M1 radiation is possible and is expected to predominate. The suggestion of the data that the radiation is E2 (E1 is forbidden for either spin assignment and will not be considered) is therefore somewhat surprising, if correct. It is a happy occurrence, however, in that E2 is only slightly less likely than M1 for a (3/2, odd) to (1/2, odd) transition but is absolutely forbidden for a (1/2, odd) to (1/2, odd) transition. The spin of the state would therefore be confirmed by that finding.

A valuable line of evidence which has been pointedly ignored in this analysis is the array of states in the mirror nucleus, N^{13}. This reticence was occasioned by the desire to develop entirely independent information on C^{13} and to let the similarities support the mirror-equality hypothesis, rather than the reverse. Actually, it is probably a little late in the season for this attitude; few propositions of nuclear theory have more overwhelming evidence in their favor than that of the equality of nn and pp forces.

A brief summary of pertinent data on N^{13} follows. It is taken mostly from the reports by the Wisconsin group[52] on proton elastic scattering from C^{12}, *though much corroborative evidence* from $C^{12}(p,\gamma)N^{13}$ exists[53]. A much more detailed survey is contained in a paper by Thomas[54] in which the levels are compared and their displacements accounted for.

Table IV compares the first four isotopic spin doublets of C^{13} - N^{13}. Resonance widths (Γ) are center of mass values. The last column gives the reduced widths in dimensionless units (θ^2) derived from the observed widths.

TABLE II

STATES OF C^{13} - N^{13}

C^{13}		N^{13}		
E_r(Mev)	spin, parity	E_r(Mev)	Γ(kev)	$\theta^2/2$
0	1/2, odd	0	-	0.035 or 0.15*
3.082 - 0.007	1/2, even	2.369	31	0.81
3.684 - 0.015	3/2, odd	3.511	55	0.047
3.843 - 0.015	5/2, even	3.558	61	0.31

*from radiative transition widths in capture of s-wave nucleons by C^{12} [54].

The quantity tabulated gives a measure of the extent to which a level may be described by a configuration involving the interaction of a single nucleon with a core. (In the formalism of dispersion theory, it measures the probability that the nucleon appears at the nuclear surface[54]). Its value should be of order one for single-particle levels and much less for levels due to appreciable excitation of the core. Thus, the 3.1- and 3.85-Mev levels appear to consist of single-particle configurations, while the 3.68-Mev level is complex.

The resonant proton capture gamma-radiation from the (3/2, odd) 3.511-Mev level in N^{13} is predominantly magnetic dipole, according to its angular distribution[53cd], and has a large radiative width. This is the only point of dissimilarity between the two nuclei, if the borderline results on the 3.68-Mev line of C^{13} stand up. The absence of a Doppler shift may suggest a lifetime some 10^2 or 10^3 times greater than that of the mirror transition. (It may, on the other hand, result from the long lifetime of the 168-kev transition feeding the level). Taken in conjunction with the internal pair data, the suggestion is that magnetic dipole radiation is somehow suppressed for this transition in C^{13} and encouraged in the mirror case. Such a finding must be explained by the nature of the multi-particle 3.68-Mev level.

REFERENCES

1. a Hornyak, Lauritsen, and Rasmussen, Phys. Rev. 76, 731 (1949);

   b W. F. Hornyak, Ph.D. Thesis, Calif. Inst. of Tech., (1949);

   c V. K. Rasmussen, Ph.D. Thesis, Calif. Inst. of Tech., (1950).

2. C. Wong, Ph.D. Thesis, Calif. Inst. of Tech., (1953).

3. a R. G. Thomas and T. Lauritsen, Phys. Rev. 88, 969 (1952);

   b R. G. Thomas, Ph.D. Thesis, Calif. Inst. of Tech., (1951).

4. C. Sharp Cook, ONR Technical Report, Washington U., Jan. 28, 1953.

5. W. L. Brown, Phys. Rev., 83, 271 (1951).

6. G. Lindström, Phys. Rev., 83, 465 (1951);

   see also: Meyer & Schmidt, Phys. Rev., 89, 908A (1953).

7. a Y. Cauchois, J. Phys. et Rad., 13, 113 (1952);

   b Hill, Church, and Mihelich, Revs. Sci. Inst., 23, 523 (1952).

8. N. Bohr, DKDVS, Mathematisk-fysiske Meddelelser 18, 8 (1948).

9. A. Bohr, DKDVS, Mathematisk-fysiske Meddelelser 24, 19 (1948).

10. L. Landau, J. Phys. USSR 8, 201 (1944).

11. D. H. Tomboulian and E. M. Pell, Phys. Rev. 83, 355 (1951).

12. J. J. L. Chen and S. D. Warshaw, Phys. Rev., 84, 355 (1951).

13. Kageyama and Nishimura, J. Phys. Soc. Japan, 7, 292 (1952).

14. F. Ajzenberg and T. Lauritsen, Revs. Mod. Phys. 24, 321 (1952).

15. Chao, Tollestrup, Fowler, and Lauritsen, Phys. Rev. 79, 108 (1950).

16. Sanders, Phil. Mag. 43, 630 (1952).

17. Hulme, McDougall, Buckingham, and Fowler, Proc. Roy. Soc. A149, 131 (1935).

18. H. Hall, Revs. Mod. Phys. 8, 395 (1936).

19. L. H. Gray, Proc. Camb. Phil. Soc. 27, 103 (1931).

20. F. Sauter, Ann. der Physik 9, 217 (1931), and 11, 454 (1931).

21. Rose, Goertzal, Spinrad, Harr, and Strong, Phys. Rev. 83, 79 (1951).

22. M. E. Rose, Phys. Rev. 76, 678 (1949); 78 184 (1950).

23. Rose and Uhlenbeck, Phys. Rev. 48, 211 (1935).

24. G. C. Phillips, Phys. Rev. 80, 164 (1950).

25. W. J. Hushley, Phys. Rev. 67, 34 (1945).

26. R. B. Day and R. L. Walker, Phys. Rev. 85, 582 (1952).

27. Hahn, Snyder, Willard, Bair, Klema, Kingston, and Green, Phys. Rev. 85, 934 (1952).

28. Manley and Millman, Phys. Rev. 51, 19 (1937).

29. Fowler, Lauritsen, and Lauritsen, Revs. Mod. Phys. 20, 236 (1948).

30. E. P. Wigner, Phys. Rev. 51, 106 (1937).

31. R. K. Adair, Phys. Rev. 87, 1041 (1952).

32. Fulbright, Bruner, Bromley, and Goldman, Phys. Rev. 88, 700 (1952).

33. S. T. Butler, Proc. Roy. Soc. (London) 208A, 559 (1951).

34. Cohen, Shafroth, Class, and Hanna, Phys. Rev. 87, 206A (1952).

35. a Lauritsen, Fowler, Lauritsen, and Rasmussen, Phys. Rev. 73, 636 (1948);

b Rasmussen, Lauritsen, and Lauritsen, Phys. Rev. 75, 199 (1949);

c Rasmussen, Hornyak, and Lauritsen, Phys. Rev. 76, 581 (1949);

d Chao, Lauritsen, and Rasmussen, Phys. Rev. 76, 582 (1949);

e V.K. Rasmussen, Ph.D. Thesis, Calif. Inst. of Tech., (1950).

36. Fay Ajzenberg, Phys. Rev. 82, 43 (1951); 88, 298 (1952).

37. Salmon, Proc. Phys. Soc. (London) 64A, 848 (1951).

38. H. T. Richards, U. of Pittsburgh, Medium-Energy Nuclear Physics Conference (1952).

39. M. Goldhaber and A. W. Sunyar, Phys. Rev. 83, 906 (1951).

40. G. Scharff-Goldhaber, Physica 18, 1105 (1952).

41. T. W. Bonner and J. W. Butler, Phys. Rev. 83, 1091 (1951).

42. L. A. Radicatti, Proc. Phys. Soc. (London) 66A, 139 (1953).

43. Meyerhof, Rhoderick, and Mann, Phys. Rev. 83, 203A (1951).

44. a J. Rotblat, Harwell Conference Report (1950).

b J. Rotblat, Nature 167, 1027 (1951).

c J. Rotblat, Phys. Rev. 83, 1271 (1951).

45. Bartholomew and Kinsey, Can. Jour. Phys. (to be published).

46. Van Patter, Buechner, and Sperduto, Phys. Rev. 82, 248 (1951).

47. Malm and Buechner, Phys. Rev. 81, 519 (1951).

48. Bockelman et al, MIT Prog. Rept. (LNS) Aug. 31, 1952).

49. a K. Marty, J. de Phys. et Rad. 13, 40 (1952).

b Kai Siegbahn, Manne Siegbahn Mem. Vol., p. 232, Almqvist and Wiksells Boktryckeri Ab, Uppsala (1951).

50. Goudsmit and Saunderson, Phys. Rev. 57, 24 (1940); 58, 39 (1940).

51. a Cuykendall, Phys. Rev. 50, 105 (1936).

b Jones, Phys. Rev. 50, 110 (1936).

52. a Jackson, Galonsky, Eppling, Hill, Goldberg, and Cameron, Phys. Rev. 89, 365 (1953).

b G. Goldhaber and R. M. Williamson, Phys. Rev. 82, 495 (1951).

c H. L. Jackson and A.I. Galonsky, Phys. Rev. 89, 370 (1953); 84, 401 (1951).

53. a W. A. Fowler and C. C. Lauritsen, Phys. Rev. 76, 314 (1949);

b J. D. Seagrave, Phys. Rev. 84, 1219 (1951);

c R. B. Day, Ph.D. Thesis, Calif. Inst. of Tech. (1951);

d R. B. Day and J. E. Perry, Jr., Phys. Rev. 81, 662 (1951).

54. R. G. Thomas, Phys. Rev. 88, 1109 (1952).

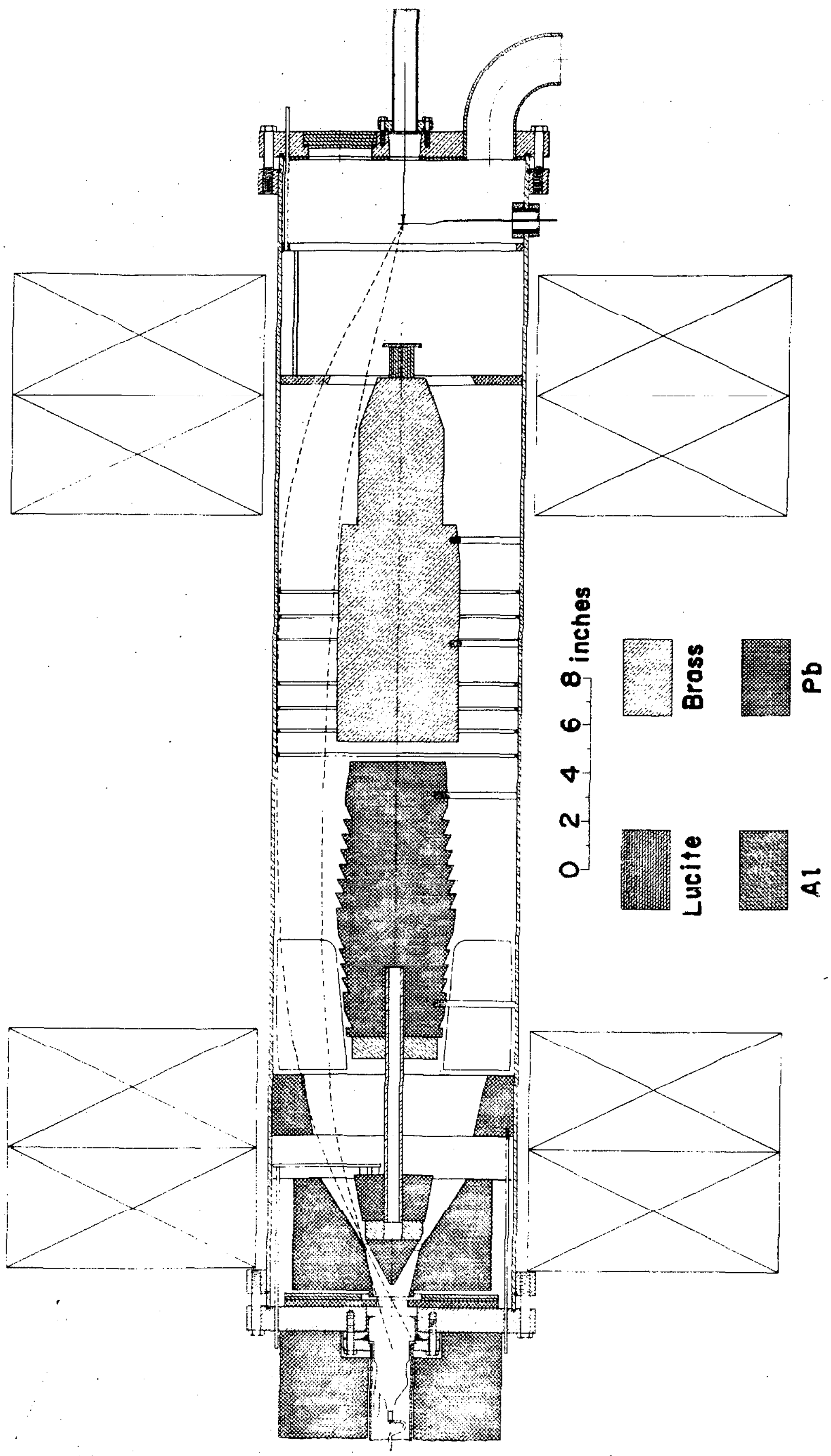

FIG. 1

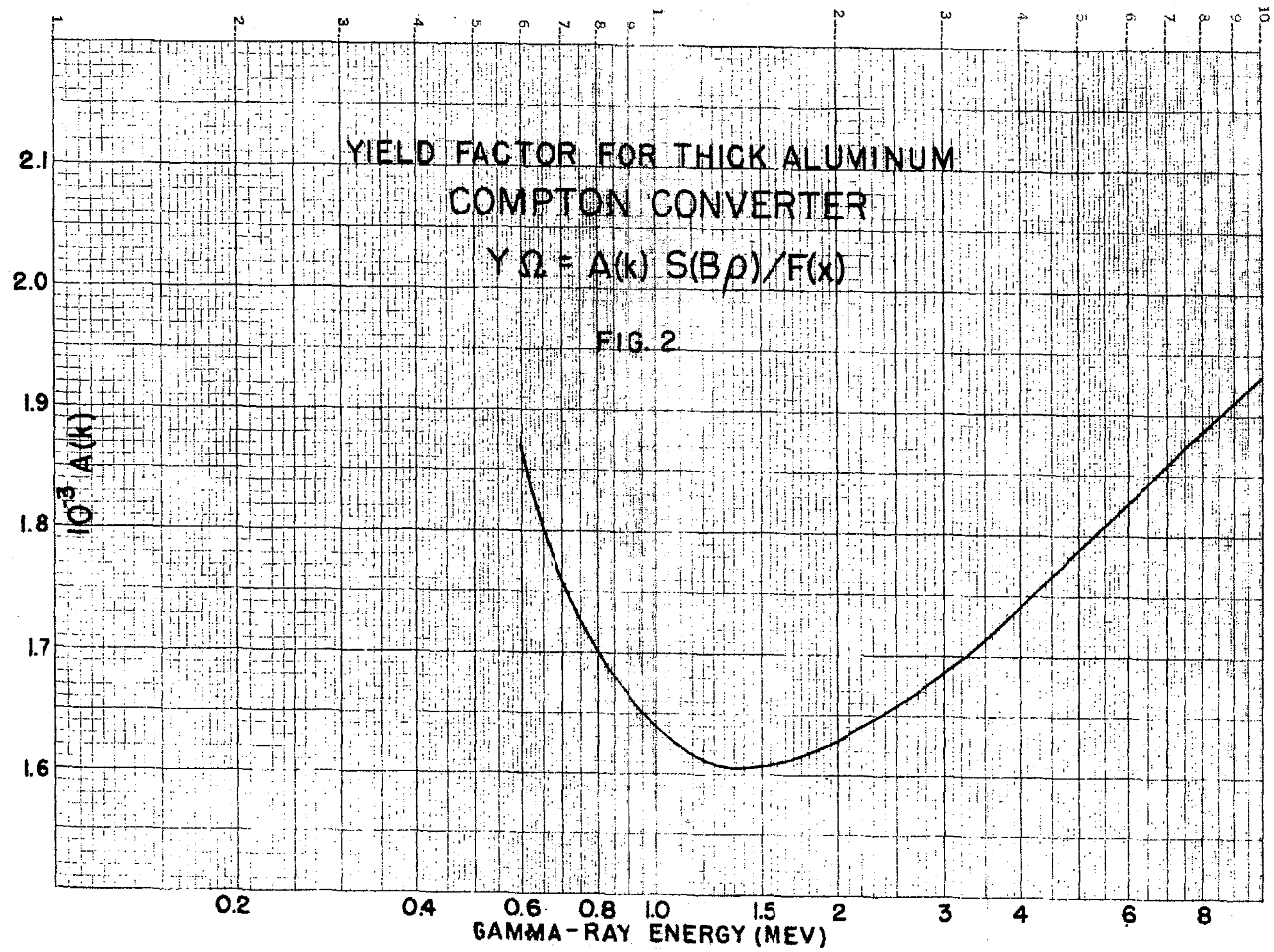
YIELD FACTOR FOR THICK ALUMINUM
COMPTON CONVERTER
Y Ω = A(k) S(Bρ)/F(x)
10^{-3} A(k)
2.1
2.0
1.9
1.8
1.7
1.6
0.2
0.4
0.6
0.8
1.0
1.5
2
3
4
6
8
GAMMA-RAY ENERGY (MEV)

FIG. 2

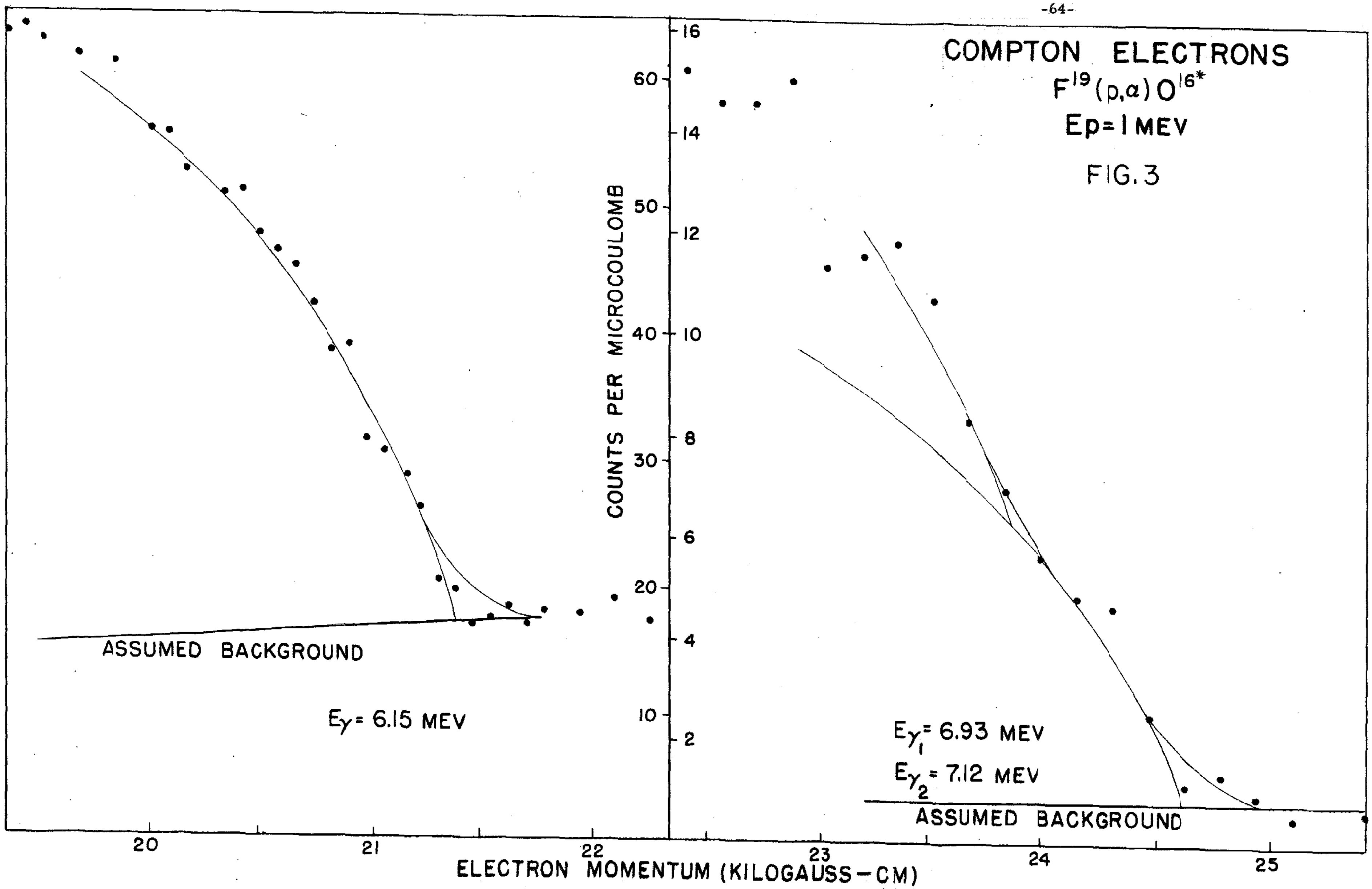

COMPTON ELECTRONS
$F^{19}(p,\alpha)O^{16*}$
Ep=1 MEV
ASSUMED BACKGROUND
E_γ = 6.15 MEV
E_{γ_1} = 6.93 MEV
E_{γ_2} = 7.12 MEV
ASSUMED BACKGROUND
COUNTS PER MICROCOULOMB
10
20
30
40
50
60
2
4
6
8
10
12
14
16
20
21
22
23
24
25
ELECTRON MOMENTUM (KILOGAUSS-CM)

FIG. 3

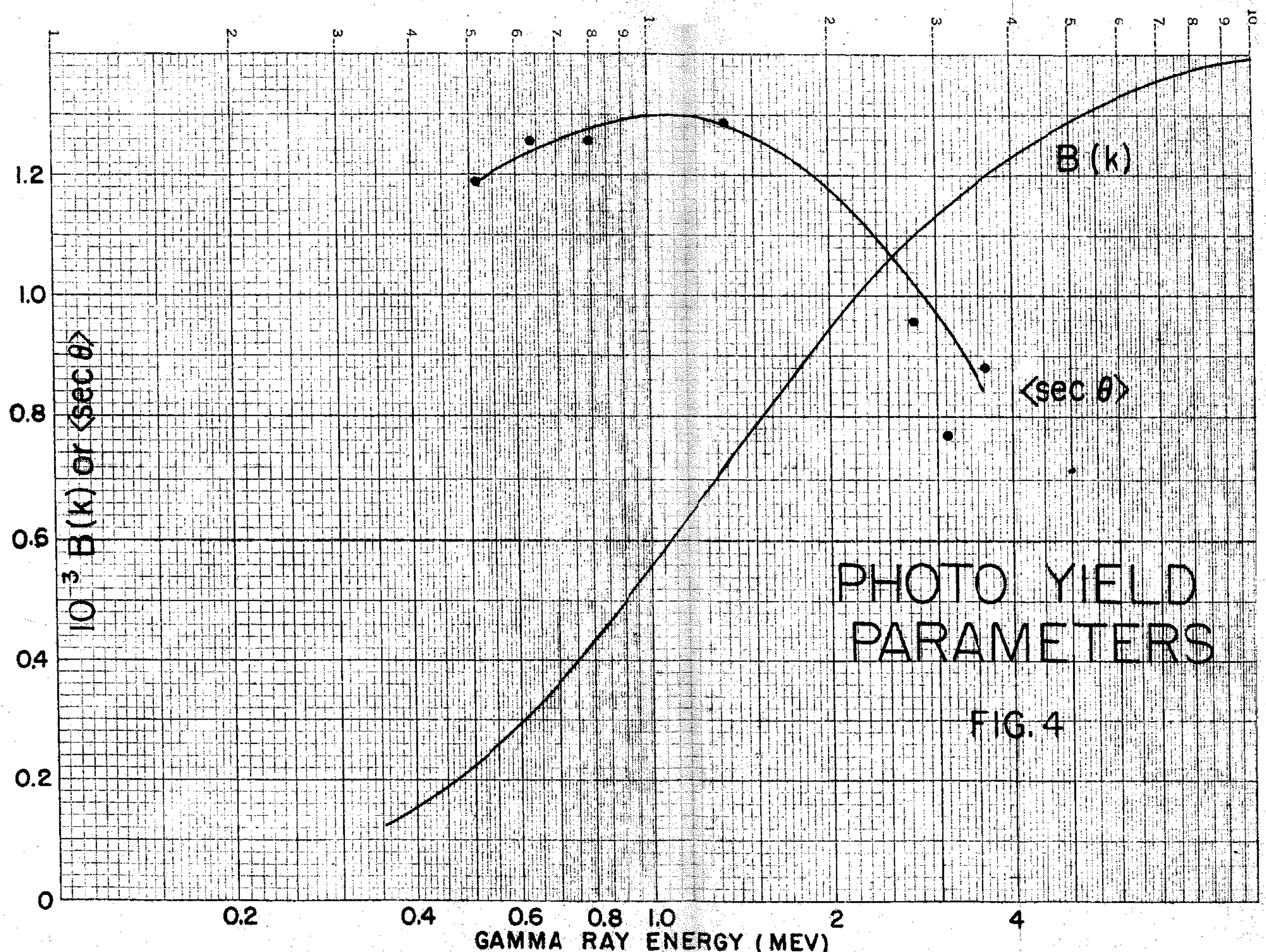

PHOTO YIELD PARAMETERS

FIG. 4

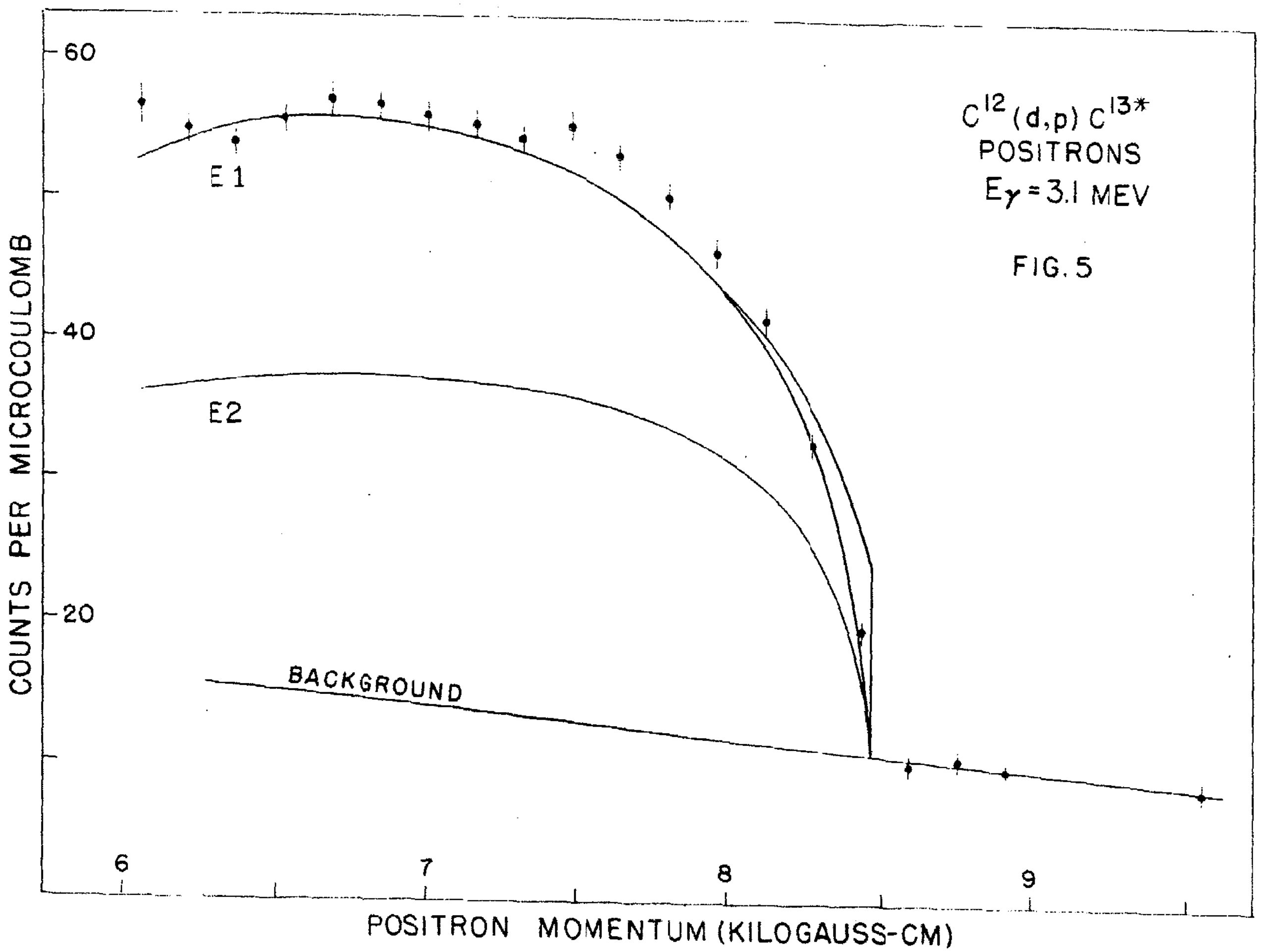
C12 (d,p) C13*
POSITRONS
Eγ = 3.1 MEV
E1
E2
BACKGROUND
COUNTS PER MICROCOULOMB
60
40
20
6
7
8
9
POSITRON MOMENTUM (KILOGAUSS-CM)

FIG. 5

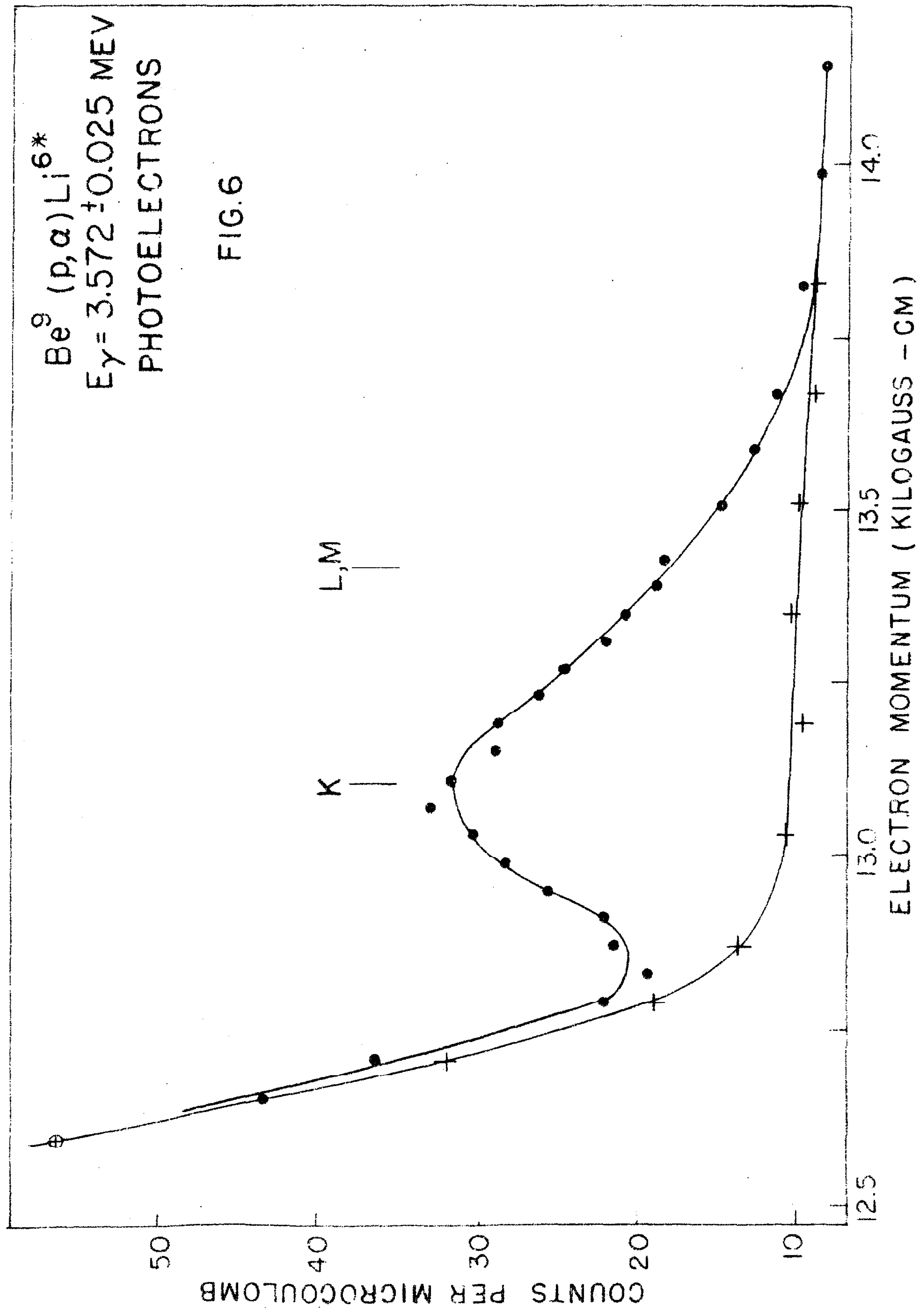

Be^{9} (p,α) Li^{6*}
E$_{\gamma}$ = 3.572 ± 0.025 MEV
PHOTOELECTRONS
FIG.6
K
L,M
COUNTS PER MICROCOULOMB
50
40
30
20
10
12.5
13.0
13.5
14.0
ELECTRON MOMENTUM (KILOGAUSS - CM)

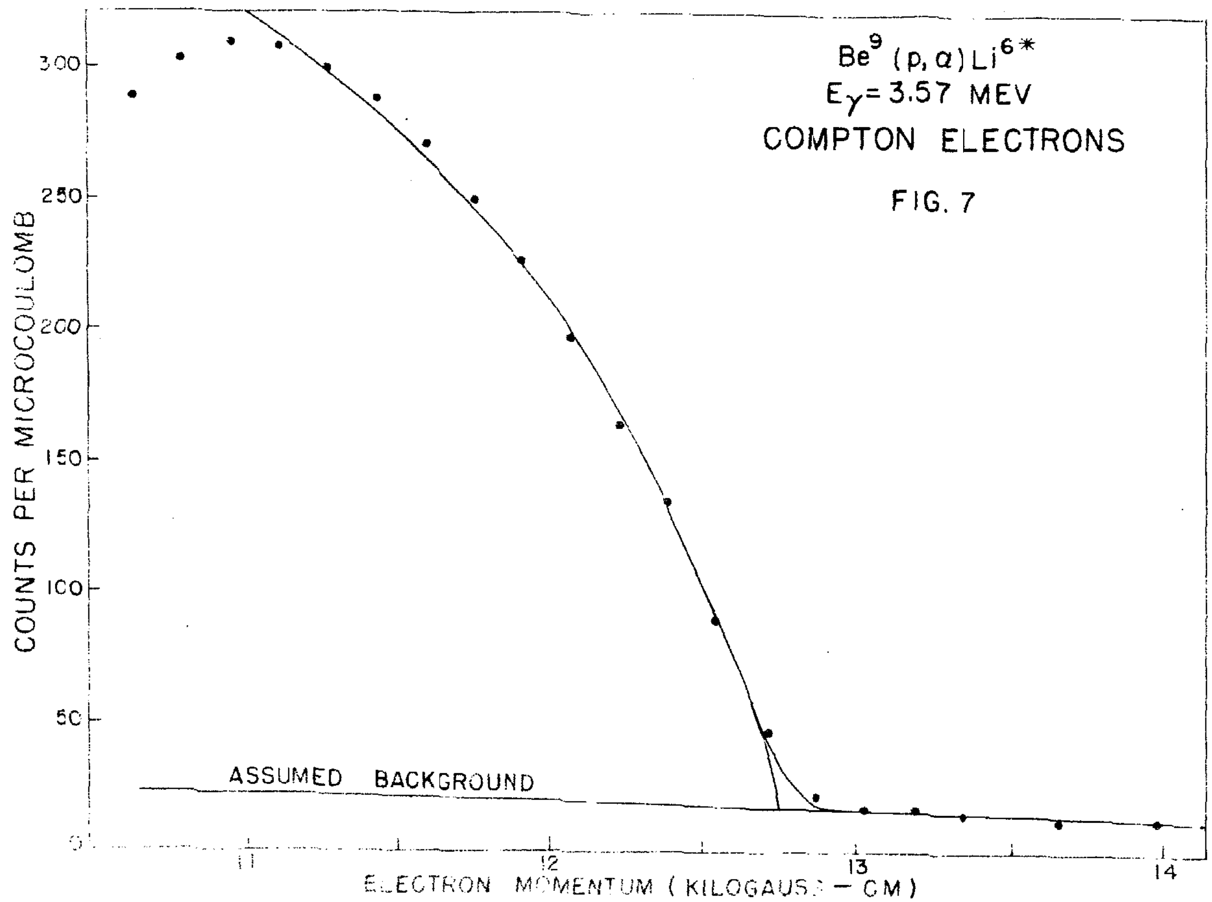

$Be^9 (p, \alpha) Li^{6*}$
$E_\gamma = 3.57$ MEV
COMPTON ELECTRONS

FIG. 7

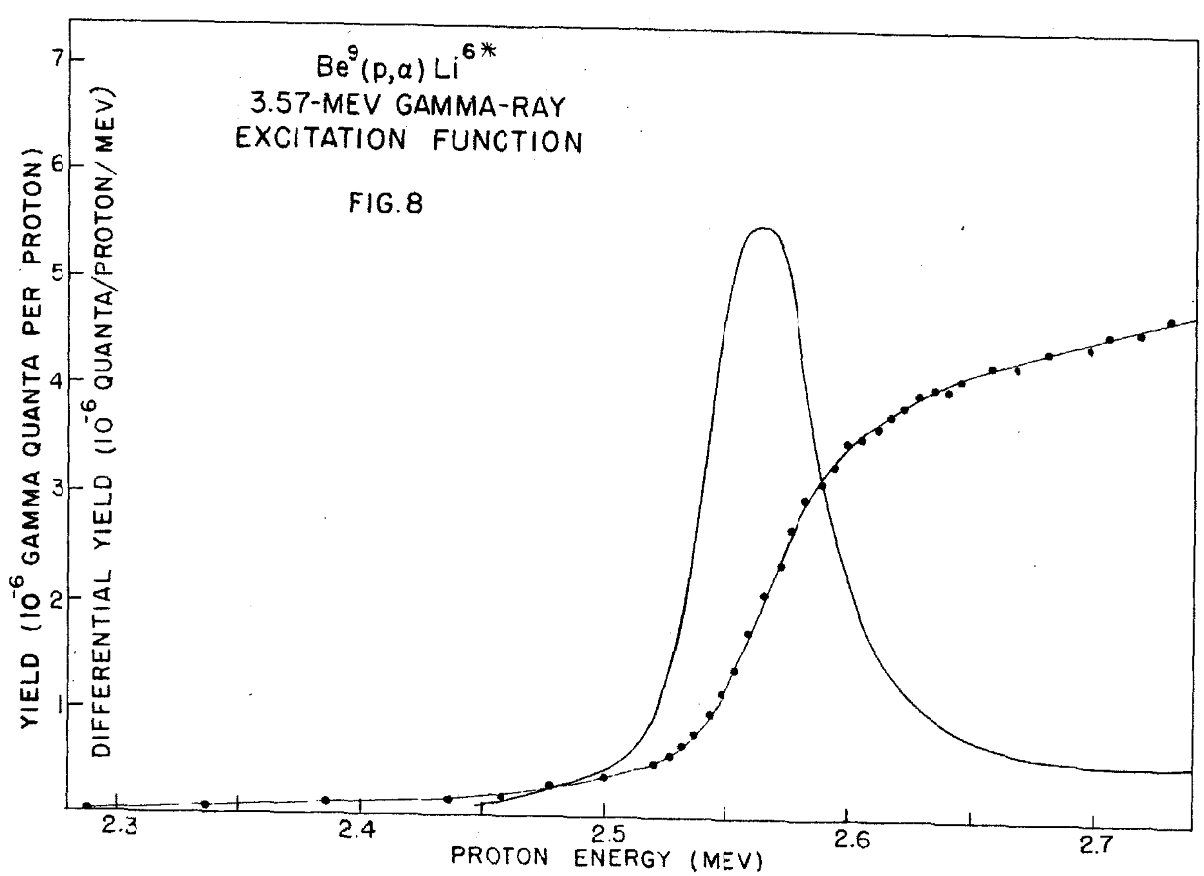

$Be^9(p,\alpha)Li^{6*}$
3.57-MEV GAMMA-RAY
EXCITATION FUNCTION
FIG. 8
YIELD (10^{-6} GAMMA QUANTA PER PROTON)
DIFFERENTIAL YIELD (10^{-6} QUANTA/PROTON/MEV)
PROTON ENERGY (MEV)
1
2
3
4
5
6
7
2.3
2.4
2.5
2.6
2.7

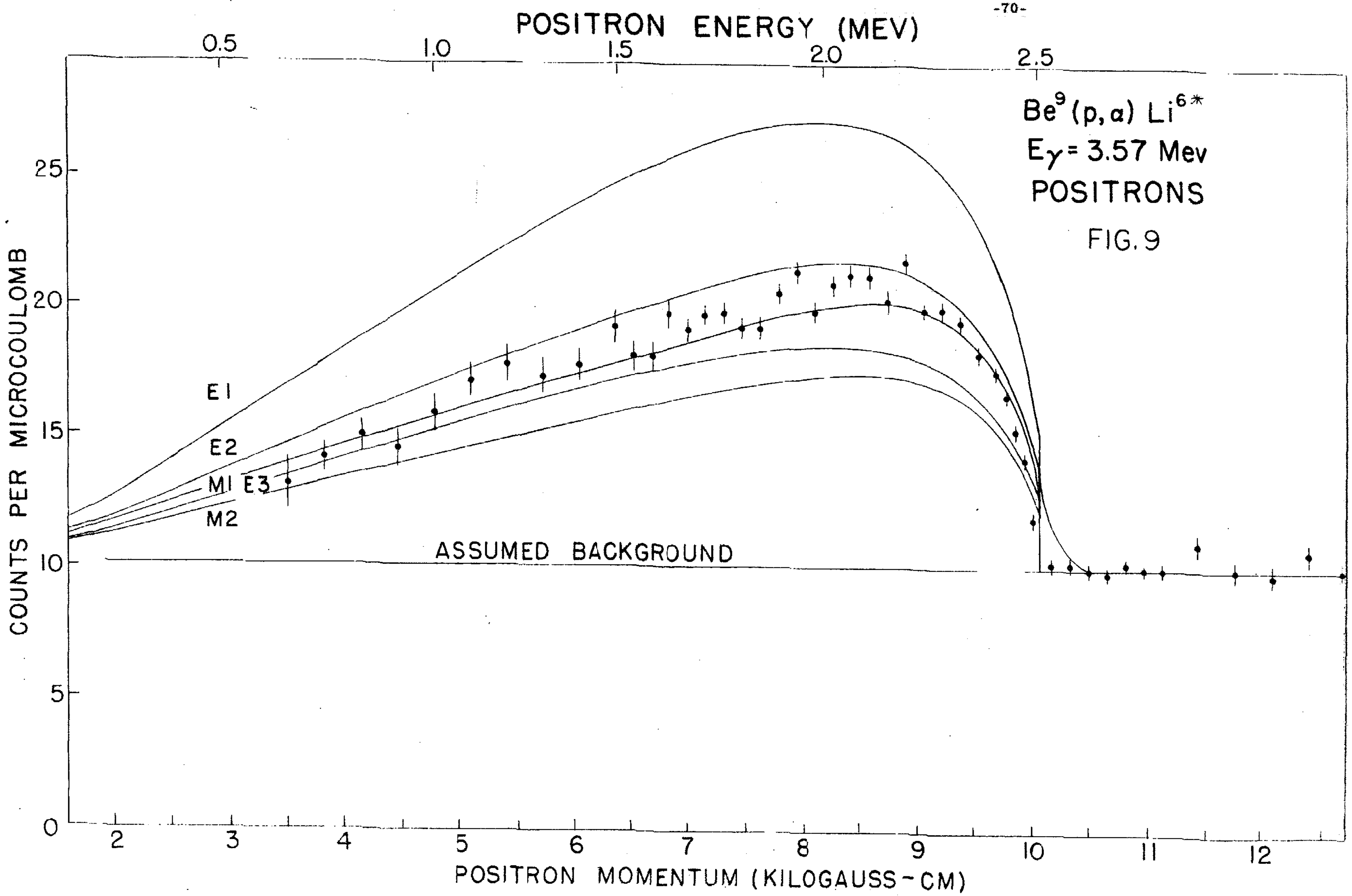
POSITRON ENERGY (MEV)
0.5
1.0
1.5
2.0
2.5
Be^9(p,α)Li^{6*}
Eγ= 3.57 Mev
POSITRONS
E1
E2
M1 E3
M2
ASSUMED BACKGROUND
COUNTS PER MICROCOULOMB
0
5
10
15
20
25
2
3
4
5
6
7
8
9
10
11
12
POSITRON MOMENTUM (KILOGAUSS-CM)

FIG. 9

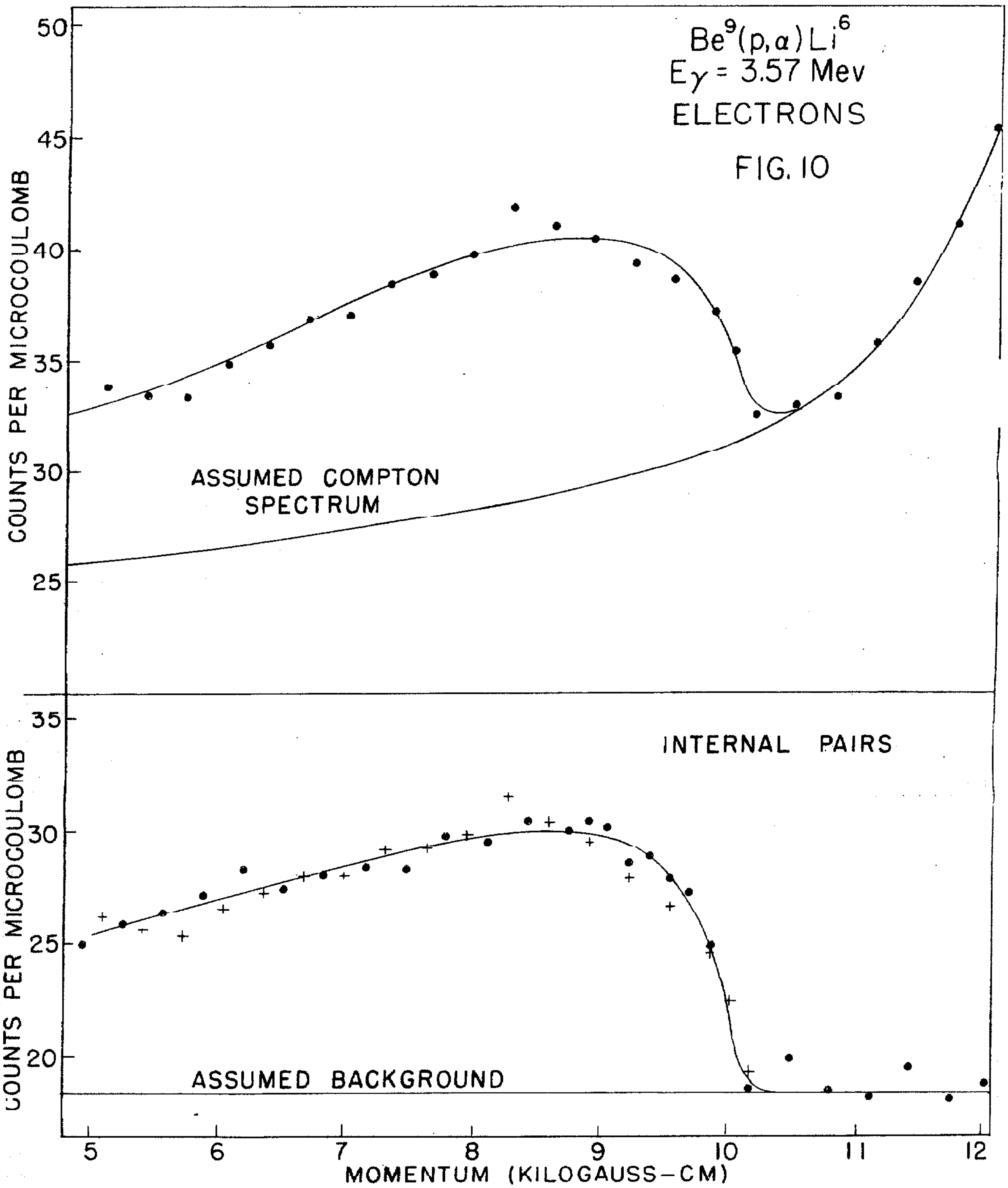

Be^{9}(p,α)Li^{6}
Eγ = 3.57 Mev
ELECTRONS
FIG. 10
ASSUMED COMPTON SPECTRUM
COUNTS PER MICROCOULOMB
50
45
40
35
30
25
INTERNAL PAIRS
ASSUMED BACKGROUND
COUNTS PER MICROCOULOMB
35
30
25
20
5
6
7
8
9
10
11
12
MOMENTUM (KILOGAUSS-CM)

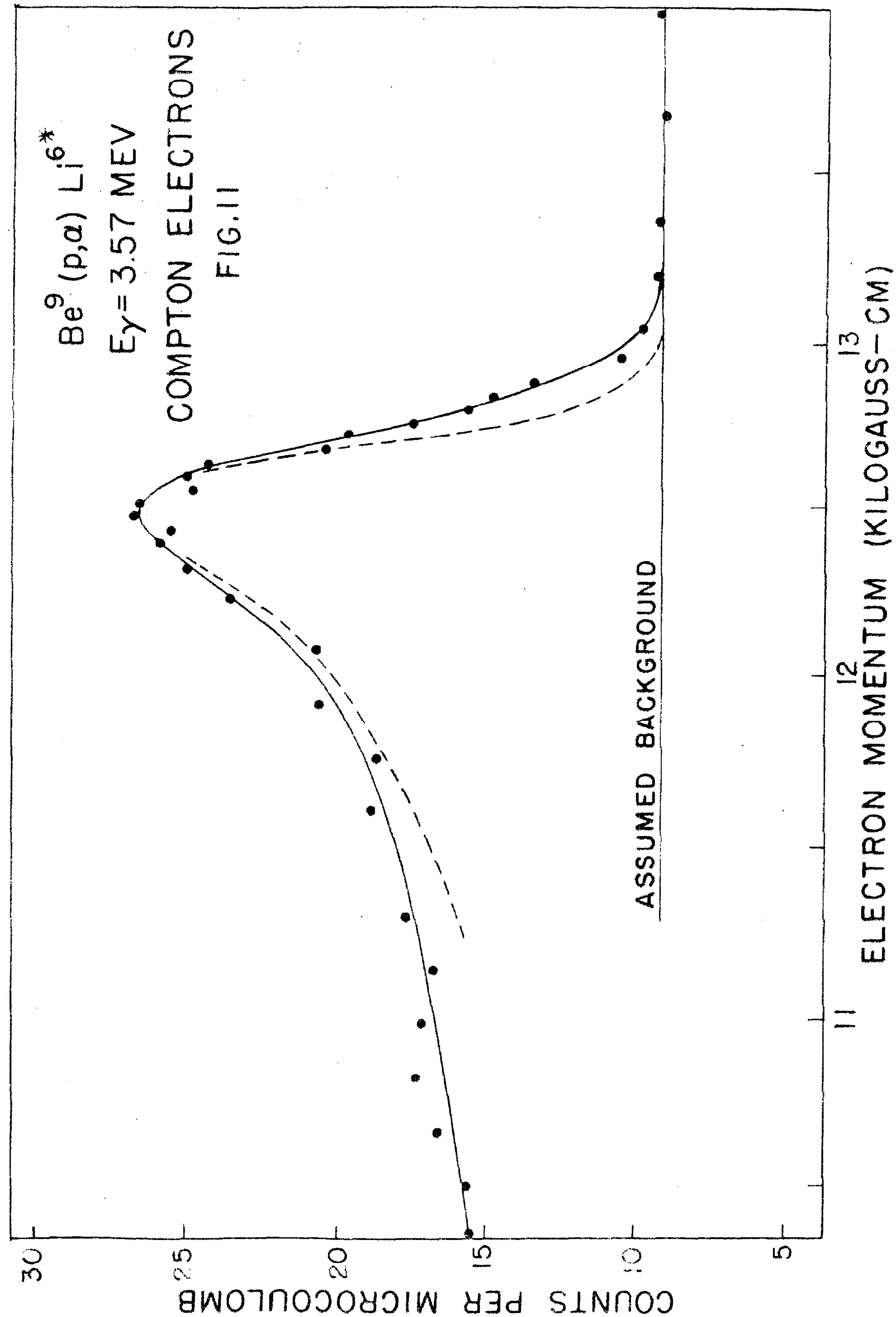

$Be^9 (p,\alpha) Li^{6*}$
$E_\gamma = 3.57$ MEV
COMPTON ELECTRONS
FIG. 11

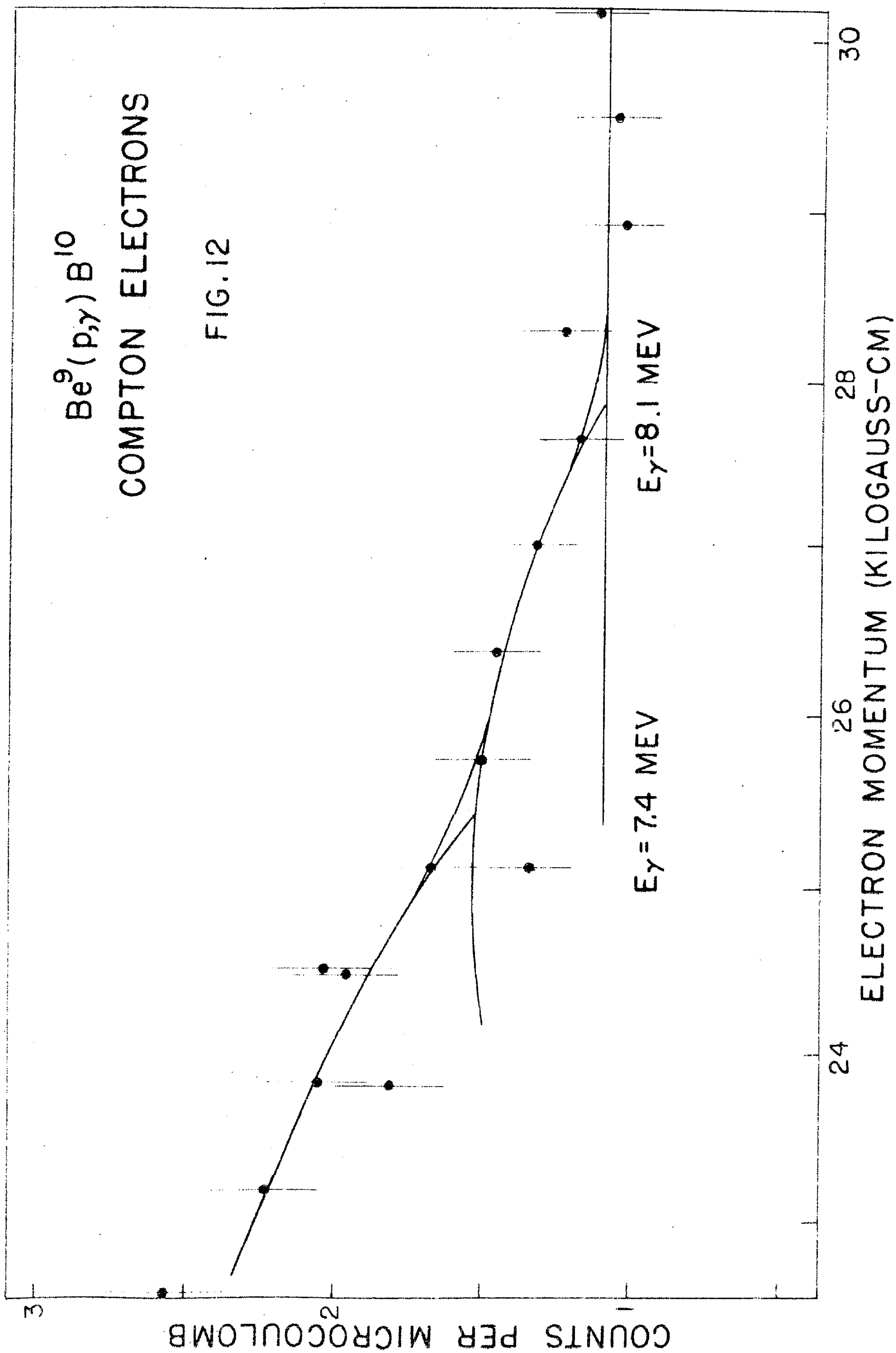
$Be^9(p,\gamma)B^{10}$
COMPTON ELECTRONS
E_γ = 7.4 MEV
E_γ = 8.1 MEV
24
26
28
30
ELECTRON MOMENTUM (KILOGAUSS-CM)
1
2
3
COUNTS PER MICROCOULOMB

FIG. 12

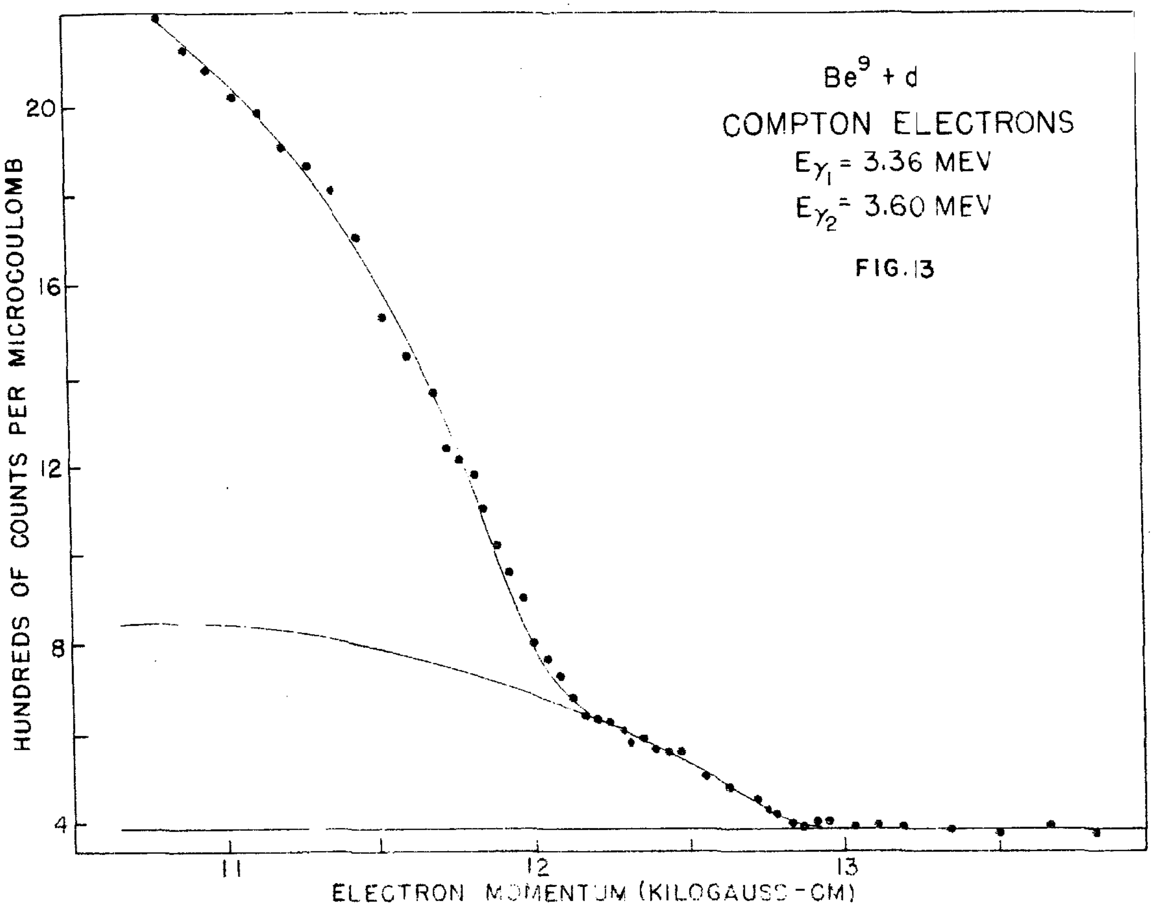

$Be^9 + d$
COMPTON ELECTRONS
E_{γ_1} = 3.36 MEV
E_{γ_2} = 3.60 MEV
HUNDREDS OF COUNTS PER MICROCOULOMB
4
8
12
16
20
11
12
13
ELECTRON MOMENTUM (KILOGAUSS-CM)

FIG. 13

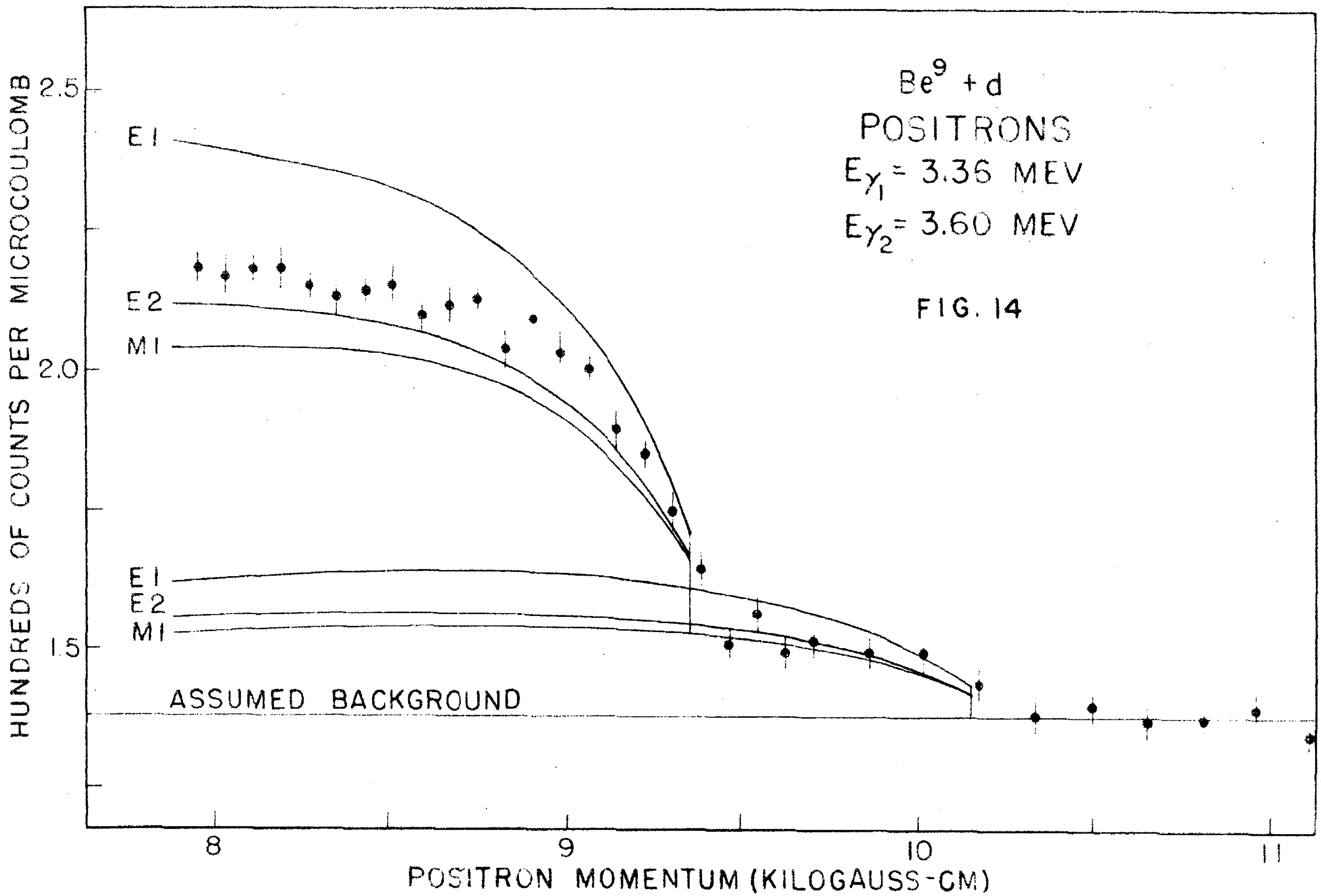
HUNDREDS OF COUNTS PER MICROCOULOMB
2.5
2.0
1.5
E1
E2
M1
E1
E2
M1
ASSUMED BACKGROUND
8
9
10
11
POSITRON MOMENTUM (KILOGAUSS-CM)
$Be^9 + d$
POSITRONS
E_{γ_1} = 3.36 MEV
E_{γ_2} = 3.60 MEV
FIG. 14

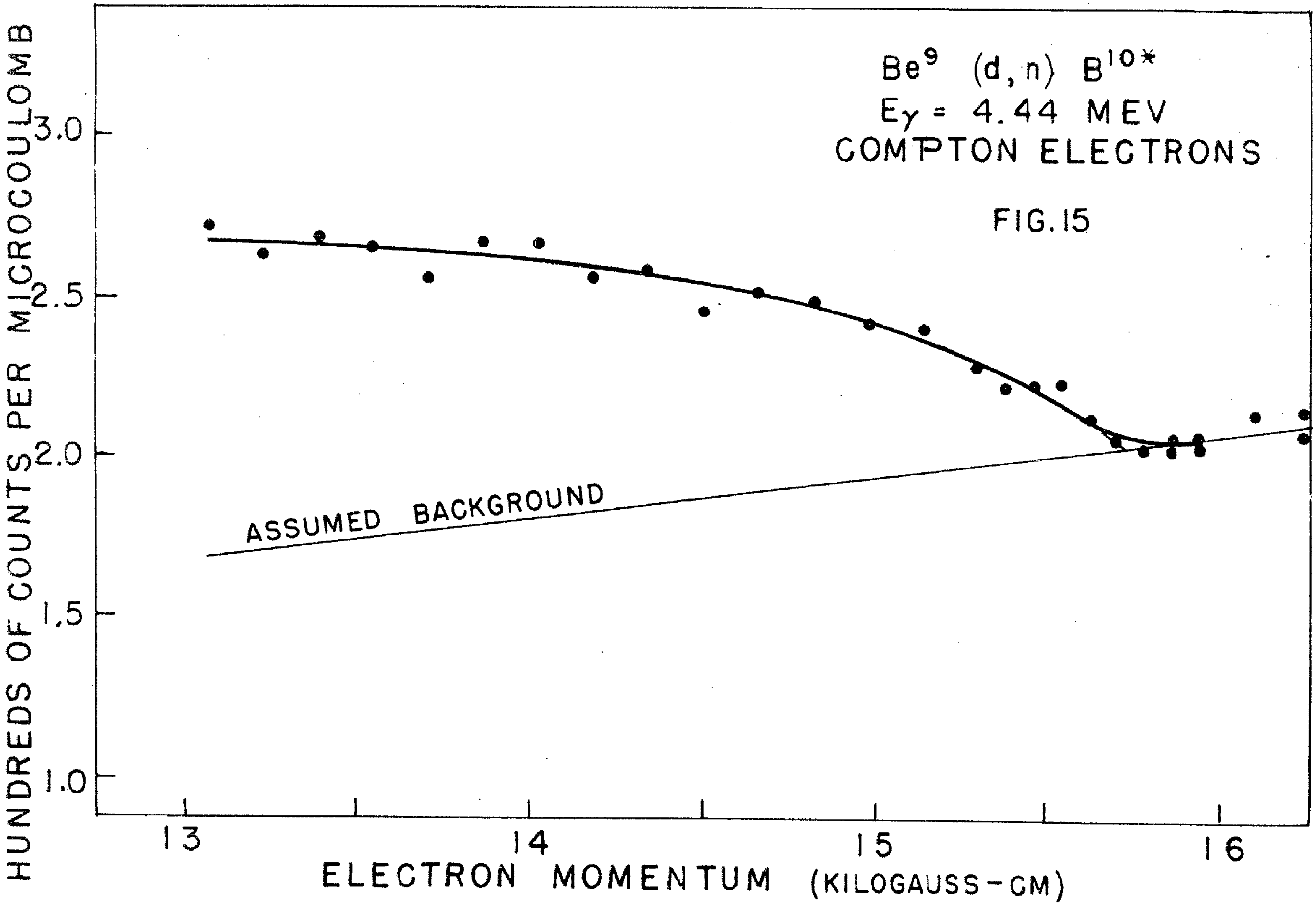
Be9 (d, n) B10*
Eγ = 4.44 MEV
COMPTON ELECTRONS
ASSUMED BACKGROUND
HUNDREDS OF COUNTS PER MICROCOULOMB
3.0
2.5
2.0
1.5
1.0
13
14
15
16
ELECTRON MOMENTUM (KILOGAUSS-GM)

FIG. 15

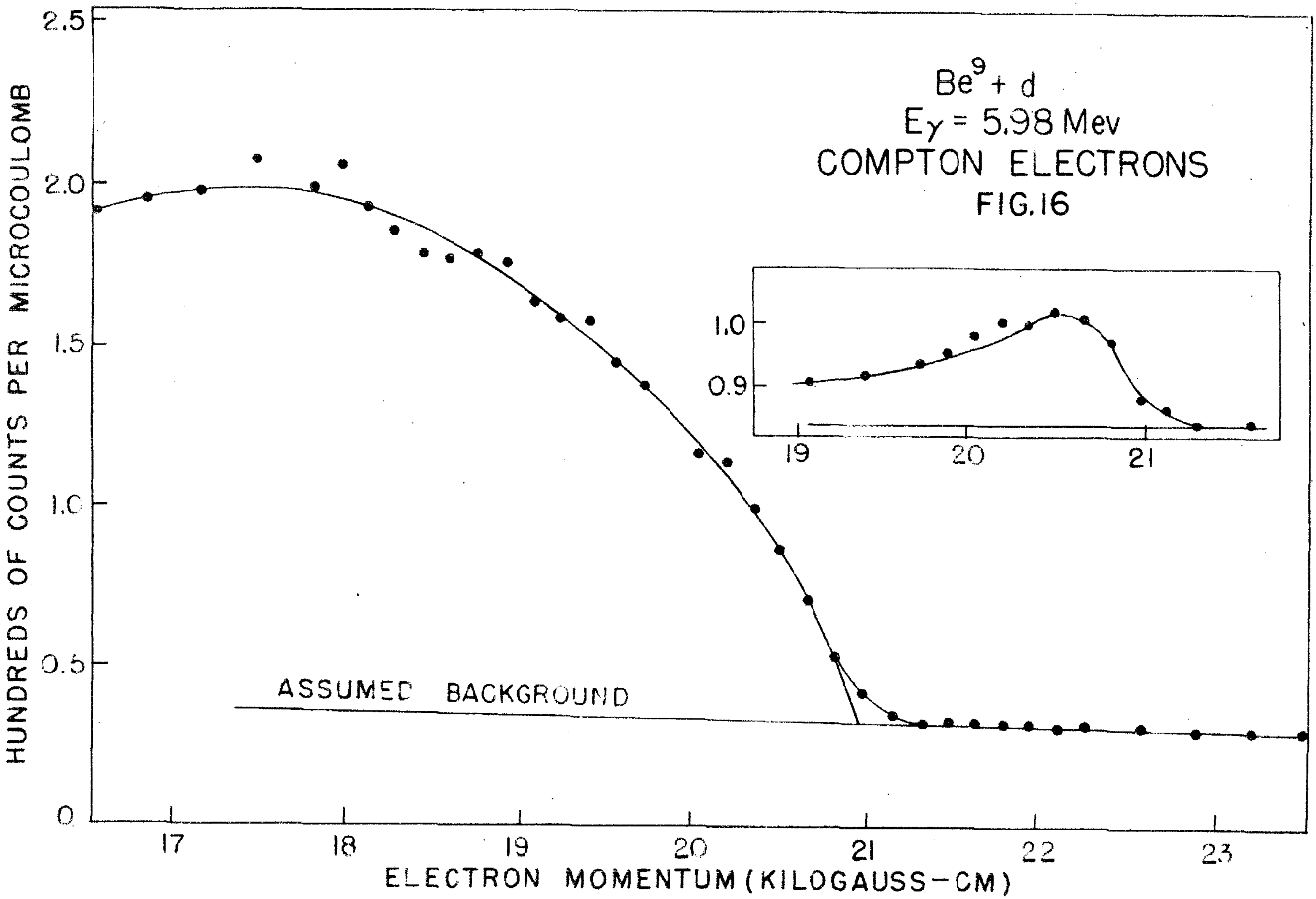

$Be^9 + d$
$E_\gamma = 5.98$ Mev
COMPTON ELECTRONS
FIG. 16

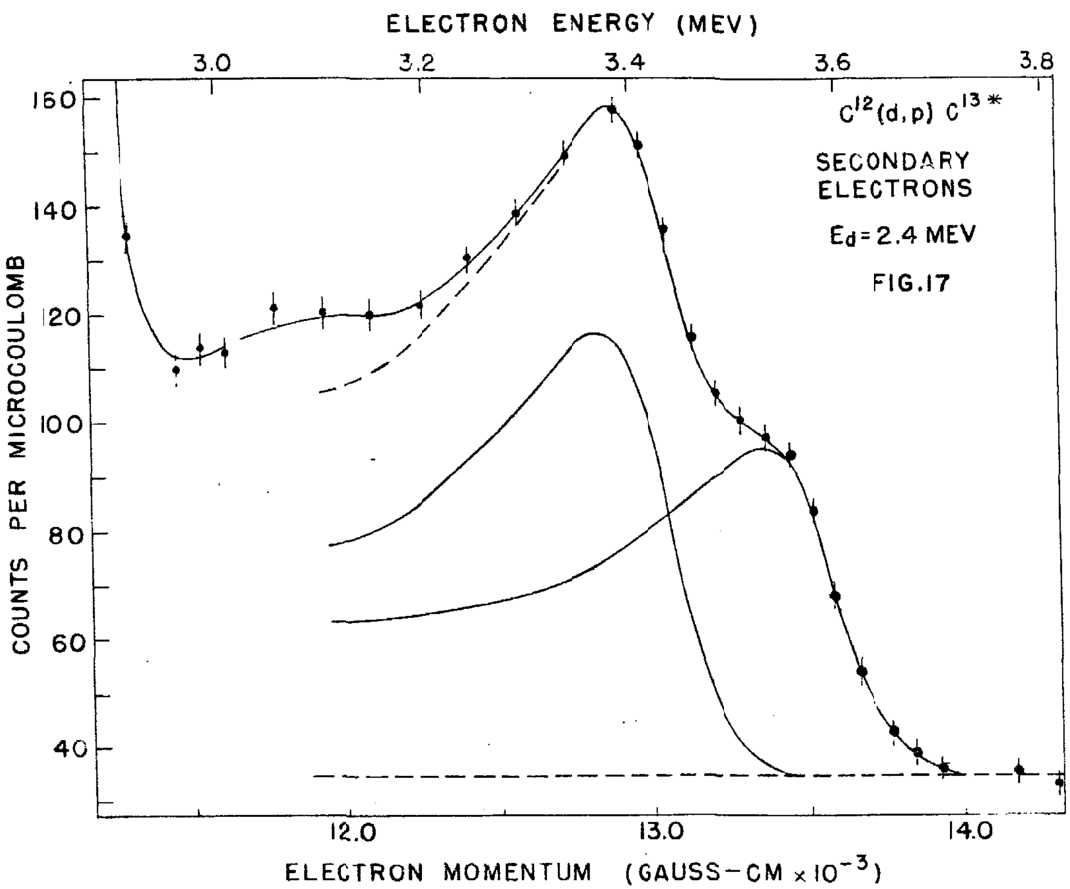
ELECTRON ENERGY (MEV)
3.0
3.2
3.4
3.6
3.8
160
140
120
100
80
60
40
COUNTS PER MICROCOULOMB
$C^{12}(d,p)\ C^{13*}$
SECONDARY
ELECTRONS
Ed = 2.4 MEV
12.0
13.0
14.0
ELECTRON MOMENTUM (GAUSS-CM × 10^{-3})

FIG.17

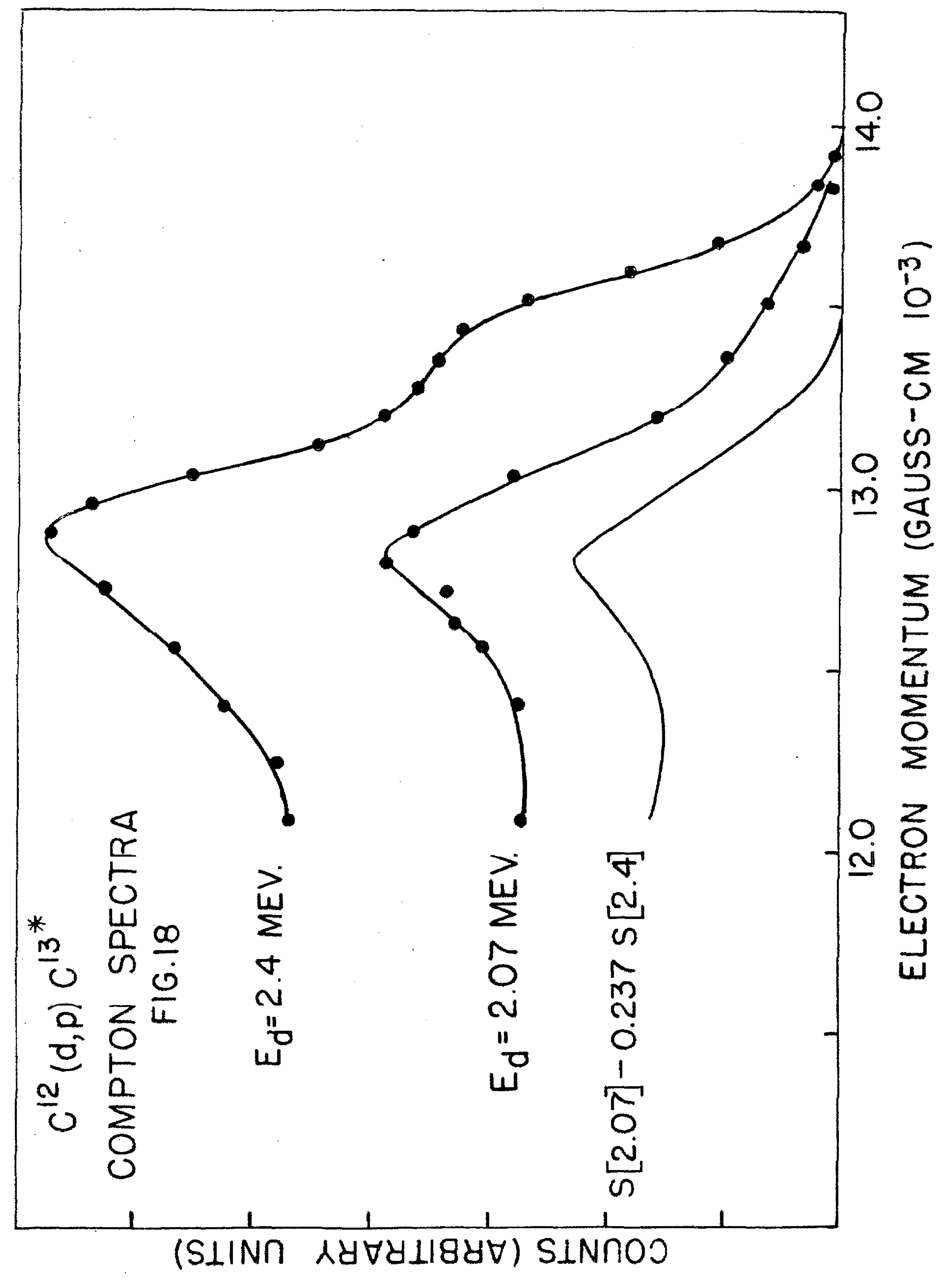

C12 (d,p) C13*
COMPTON SPECTRA
FIG. 18
Ed = 2.4 MEV.
Ed = 2.07 MEV.
S[2.07] − 0.237 S[2.4]
12.0
13.0
14.0
ELECTRON MOMENTUM (GAUSS-CM 10-3)
COUNTS (ARBITRARY UNITS)

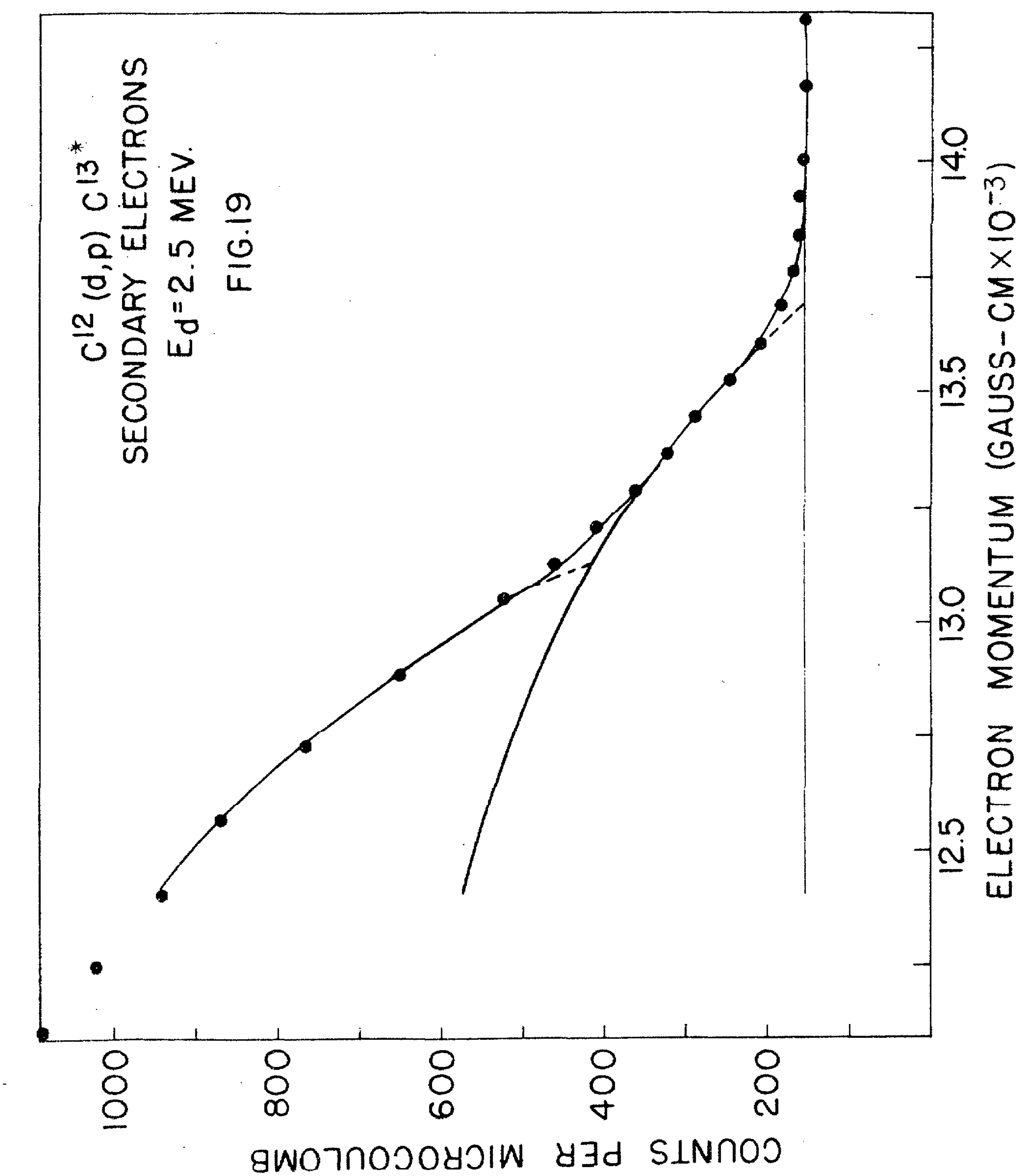

C^{12} (d,p) C^{13*}
SECONDARY ELECTRONS
E_d=2.5 MEV.
FIG. 19
COUNTS PER MICROCOULOMB
1000
800
600
400
200
12.5
13.0
13.5
14.0
ELECTRON MOMENTUM (GAUSS-CM×10⁻³)

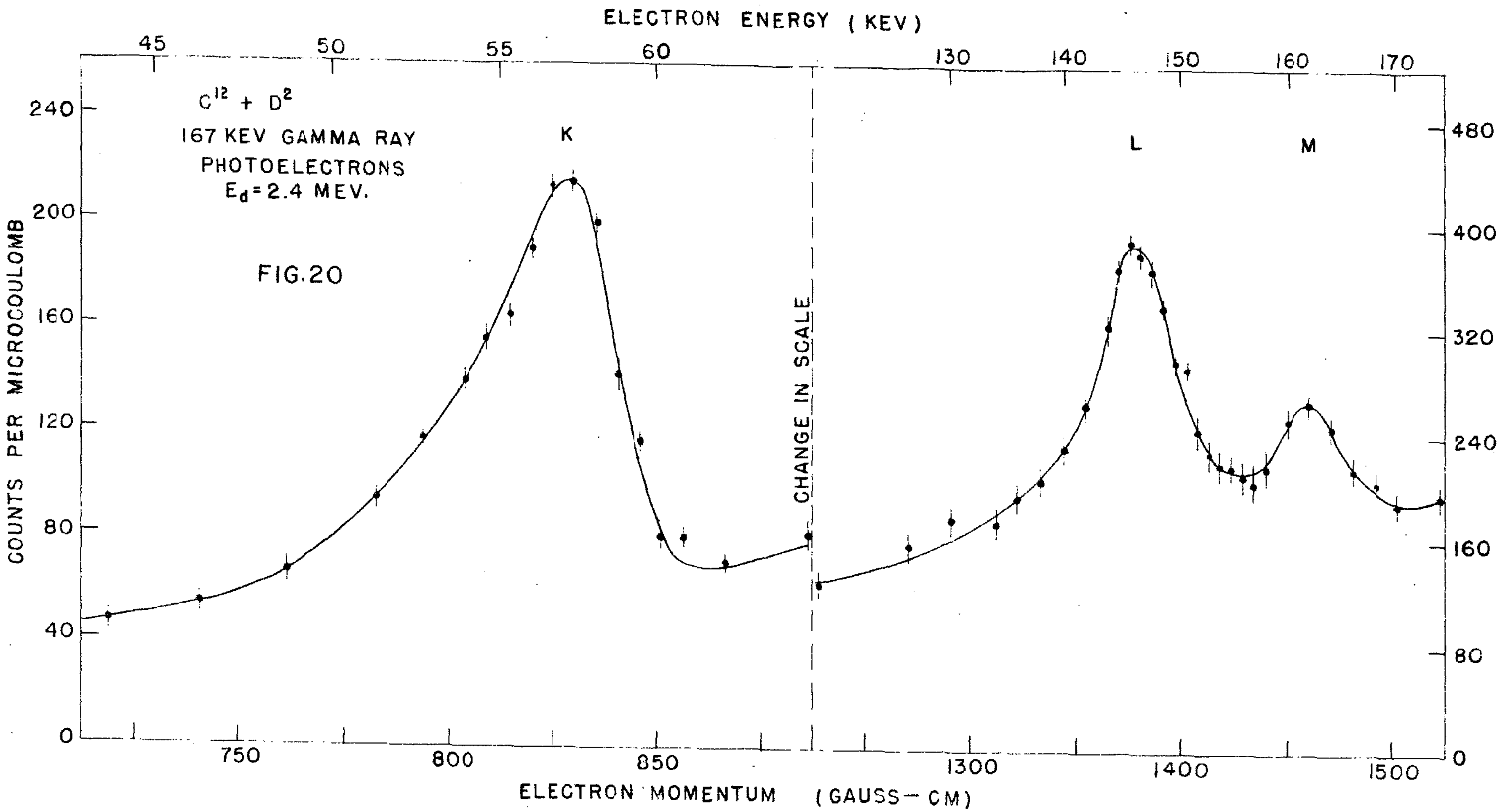
ELECTRON ENERGY (KEV)
45
50
55
60
130
140
150
160
170
$C^{12} + D^2$
167 KEV GAMMA RAY
PHOTOELECTRONS
E_d = 2.4 MEV.
K
L
M
CHANGE IN SCALE
COUNTS PER MICROCOULOMB
0
40
80
120
160
200
240
0
80
160
240
320
400
480
750
800
850
1300
1400
1500
ELECTRON MOMENTUM (GAUSS — CM)

FIG.20

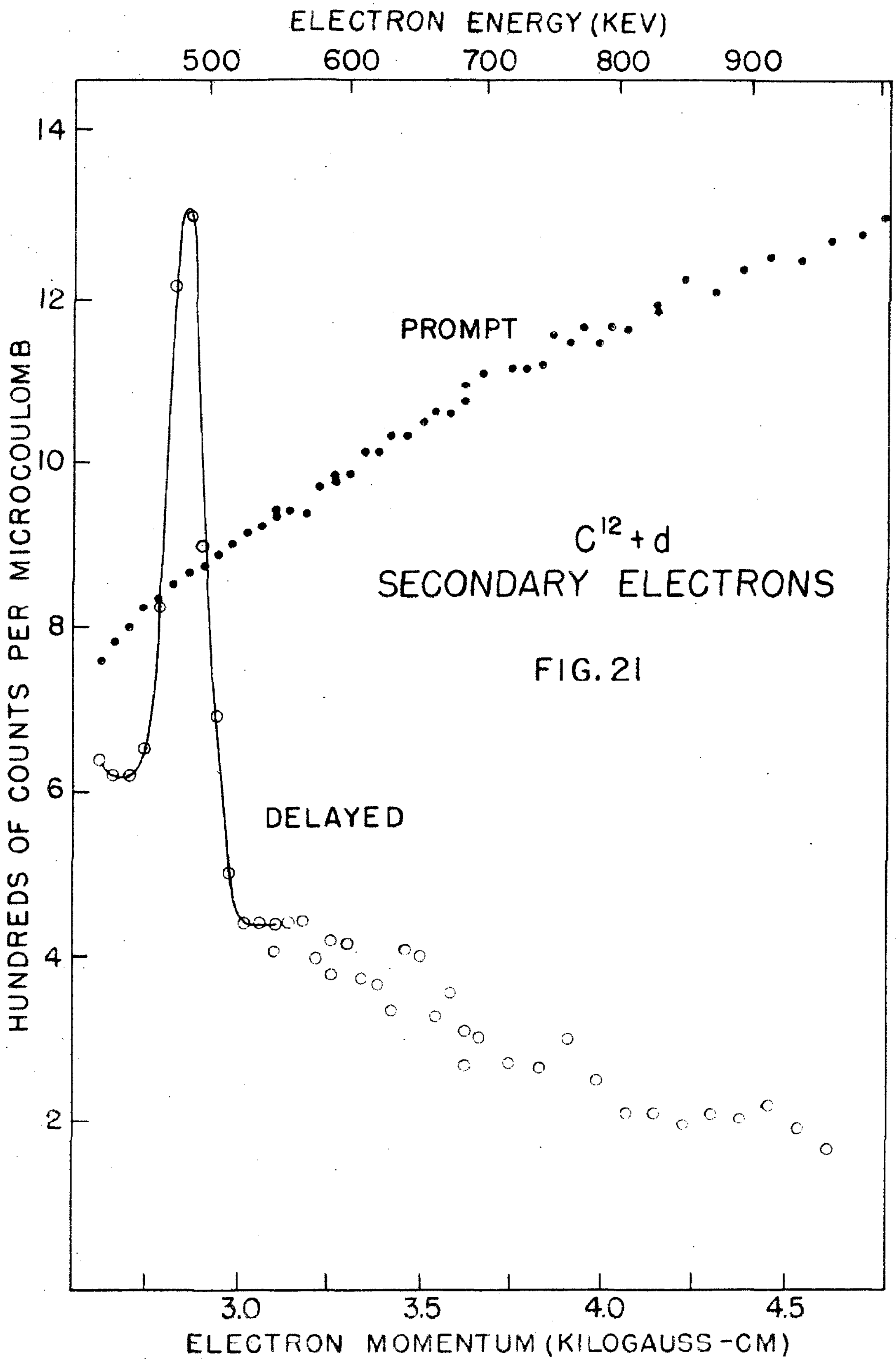
ELECTRON ENERGY (KEV)
500
600
700
800
900
14
12
10
8
6
4
2
HUNDREDS OF COUNTS PER MICROCOULOMB
PROMPT
DELAYED
$C^{12}+d$
SECONDARY ELECTRONS
3.0
3.5
4.0
4.5
ELECTRON MOMENTUM (KILOGAUSS-CM)

FIG. 21

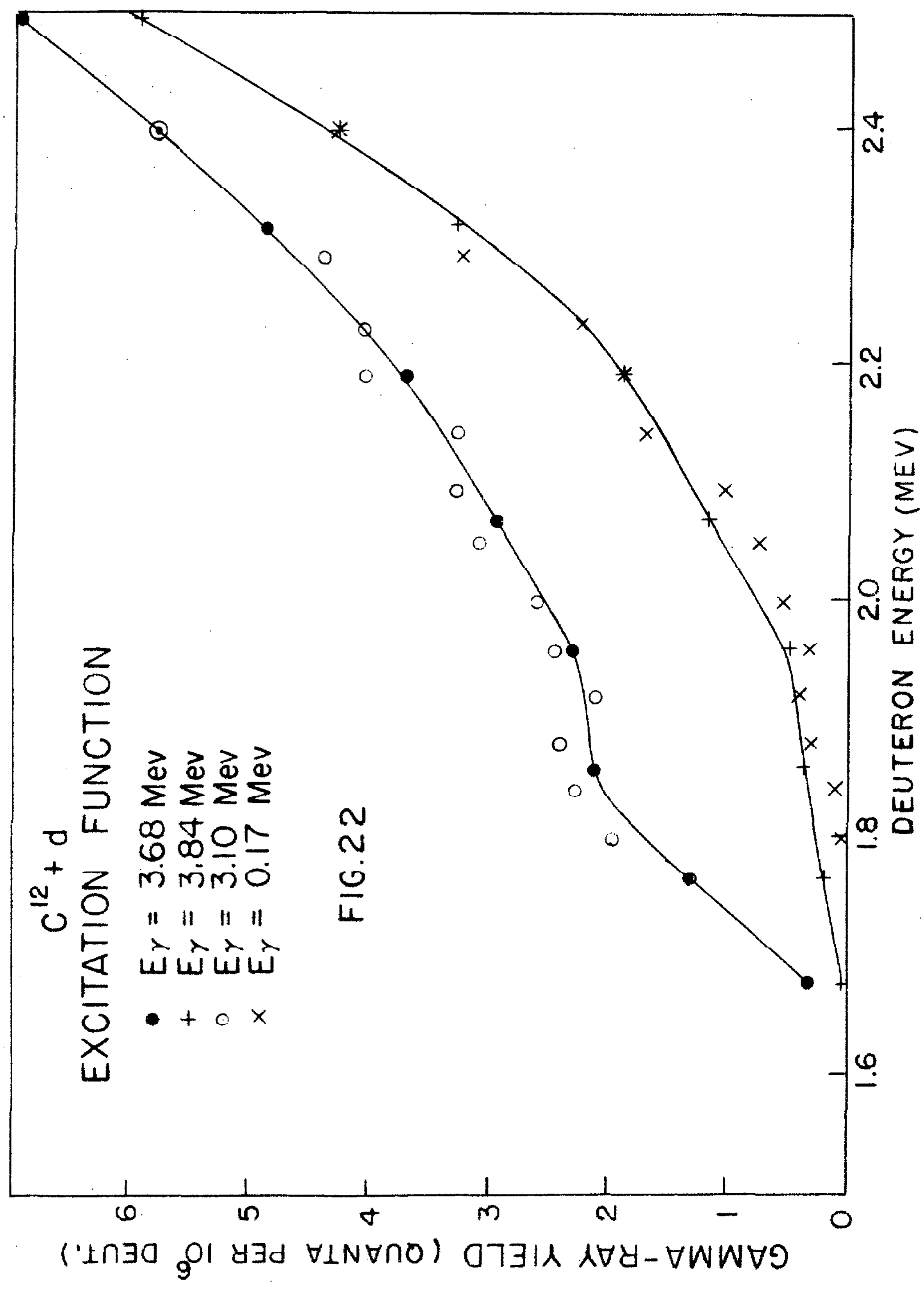

C^{12} + d
EXCITATION FUNCTION
● Eγ = 3.68 Mev
+ Eγ = 3.84 Mev
○ Eγ = 3.10 Mev
× Eγ = 0.17 Mev
DEUTERON ENERGY (MEV)
1.6
1.8
2.0
2.2
2.4
GAMMA-RAY YIELD (QUANTA PER 10^6 DEUT.)
0
1
2
3
4
5
6

FIG.22

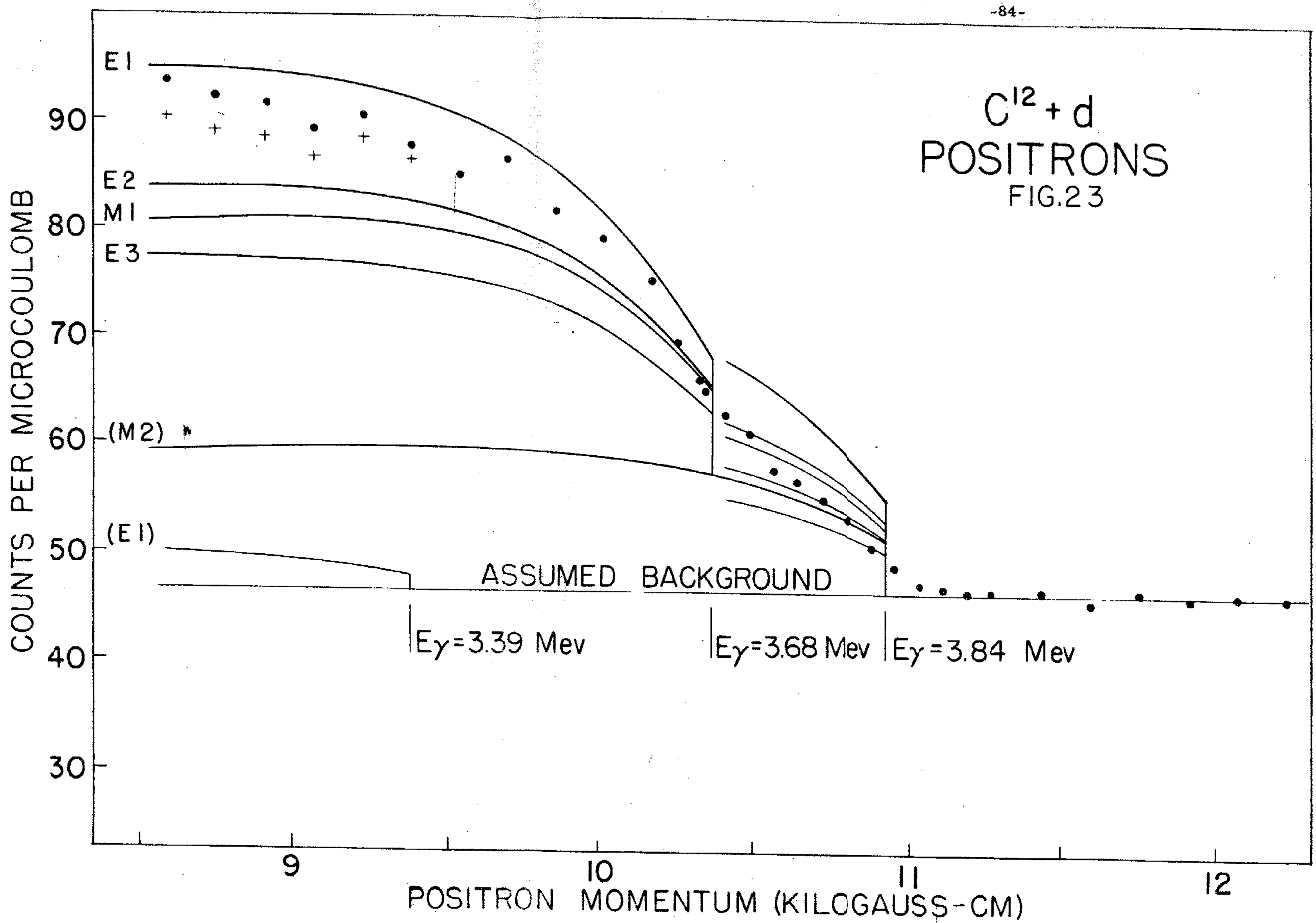
C12 + d
POSITRONS
FIG.23
COUNTS PER MICROCOULOMB
POSITRON MOMENTUM (KILOGAUSS-CM)
E1
E2
M1
E3
(M2)
(E1)
ASSUMED BACKGROUND
Eγ=3.39 Mev
Eγ=3.68 Mev
Eγ=3.84 Mev
30
40
50
60
70
80
90
9
10
11
12